

SUPPORTING INFORMATION

β -Carboline-based light and pH dual stimuli-responsive ion transporters induce cancer cell death

Mrinal Kanti Kar,^[a] Rumpa Mahata,^{[b]‡} Soumya Srimayee,^{[a]‡} Nandan Haloi,^[c, d] Rahul Kumar,^[a] Erik Lindahl,^[c,d] Manas Kumar Santra,^[b] and Debasis Manna*^[a]

.....

[a] M. K. Kar, S. Srimayee, R. Kumar, Prof. Dr. D. Manna

Department of Chemistry

Indian Institute of Technology Guwahati

Assam, 781039, India

E-mail: dmanna@iitg.ac.in

[b] R. Mahata, Prof. M. K. Santra

National Centre for Cell Science

Maharashtra, 411007, India

[c] N. Haloi, Prof. Dr. Erik Lindahl

Department of Applied Physics

Science for Life Laboratory

KTH Royal Institute of Technology

Tomtebodavägen 23, Solna, SE-17165, Sweden

[d] N. Haloi, Prof. Dr. Erik Lindahl

Department of Biochemistry and Biophysics, Science for Life

Laboratory, Stockholm University, Tomtebodavägen 23, Solna,

SE-17165, Sweden

EXPERIMENTAL SECTION

1. General Methods:

All chemical reactions were performed under an inert atmosphere. All reagents and solvents for synthesis were purchased from commercial sources (Sigma Aldrich, TCI) and used further without purification. The column chromatography was carried out using silica (60-120 mesh and 100-200 mesh). Thin-layer chromatography was performed on 60-F254 silica gel plates. Egg yolk phosphatidylcholine (EYPC) as a solution of chloroform (25 mg/ mL), mini extruder, and polycarbonate membrane of 100 nm and 200 nm were purchased from Avanti Polar Lipid. Cholesterol, HEPES, HPTS, lucigenin, Triton X-100, valinomycin, DMSO, and all inorganic salts were obtained as molecular biology grade from Sigma Aldrich. The ^1H NMR spectra and ^{13}C NMR spectra were recorded at 600 MHz. The residual solvent signals were considered as an internal reference (^1H NMR c: δ_{ppm} 7.26; ^{13}C NMR CDCl_3 : δ_{ppm} 77.2; ^1H NMR $\text{DMSO}-d_6$: δ_{ppm} 2.54; ^{13}C NMR $\text{DMSO}-d_6$: δ_{ppm} 39.5) to calibrate spectra. The chemical shifts were reported in ppm. The following abbreviations were used to indicate multiplicity patterns m: multiplet, s: singlet, d: doublet, t: triplet, q: quartet, dd: doublet of doublet, ddd: doublet of doublet of doublet, td: triplet of doublet, dt: doublet of triplet. Coupling constants were measured in Hz. High-resolution mass spectra (HRMS) were recorded on electrospray ionization time-of-flight (ESI-TOF). Fluorescence experiments were recorded on Fluoromax-4 from HORIBA, which was equipped with an injector port and magnetic stirrer in a microfluorescence cuvette. All buffer solutions were prepared from the autoclaved water. The pH of buffer solutions was adjusted using the Helmer pH meter. The extravesicular dye was removed by performing gel chromatography using Sephadex G-50. The fluorescence studies were conducted using Origin 6.0.

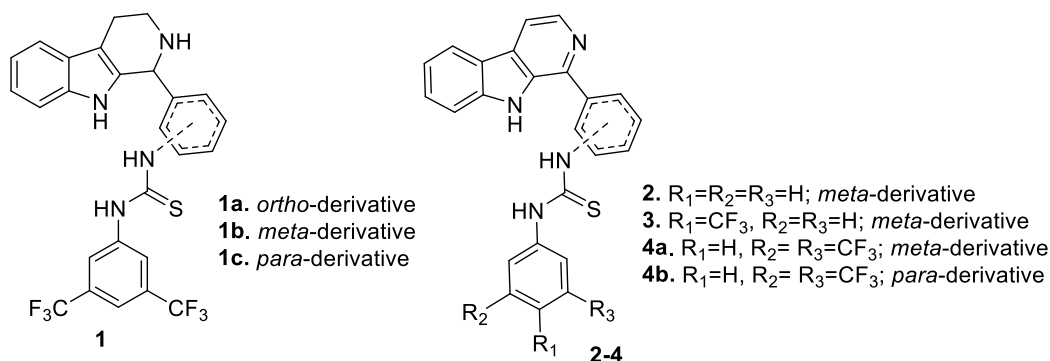
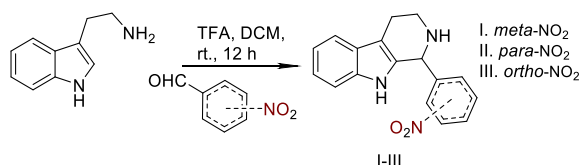
2. Estimation of logP and calculation of pK_a values:

Table S1. The estimated logP and calculated pK_a values of compounds.

Compound	Substitution	R ₁	R ₂	R ₃	logP	pK _a
1a	<i>ortho</i>	-	-	-	6.35	-
1b	<i>meta</i>	-	-	-	6.35	-
1c	<i>para</i>	-	-	-	6.35	-
2	<i>meta</i>	H	H	H	5.01	5.87
3	<i>meta</i>	CF ₃	H	H	5.94	5.78
4a	<i>meta</i>	H	CF ₃	CF ₃	6.86	5.78
4b	<i>para</i>	H	CF ₃	CF ₃	6.86	5.83

The values of logP of compounds were estimated using ChemDraw21.0.0 software, whereas the pK_a values were measured by UV-Vis studies.

3. Synthesis and characterization of the compounds:

**Scheme S1.** Synthesis of the tetrahydro β -carboline compounds.

3.1.1. General method for synthesis of tetrahydro β -carboline compounds (Pictet-Spengler reaction) — To a solution of tryptamine (500 mg, 3.12 mmol) and nitro benzaldehyde (3.12 mmol) in dichloromethane (8 mL), trifluoroacetic acid (0.5 mL) was added. The resulting mixture was stirred at room temperature overnight, and the reaction was monitored through TLC. The solution was neutralized by adding a saturated aqueous solution of NaHCO₃. The organic layer was isolated, washed with brine, and dehydrated using anhydrous sodium sulfate. The solvent was evaporated, and the product 1-substituted 1,2,3,4-tetrahydro β -carboline was obtained by column chromatography on silica gel (60-120 mesh) with 1% MeOH/ CH₂Cl₂ as an eluent (Scheme S1).¹

3.1.2. Synthesis of 1-(3-nitrophenyl)-2,3,4,9-tetrahydro-1H-pyrido[3,4-b]indole (I) — Tryptamine and *meta*-nitro benzaldehyde were used in the reaction following general protocol mentioned above. The crude reaction mixture was purified through column chromatography with a solvent gradient system of CH₂Cl₂/MeOH (0-2%) to obtain a yellow solid compound

with a 60% yield. Characterization: $^1\text{H NMR}$ (600 MHz, Chloroform-*d*) δ 8.23 (s, 1H), 8.18 (ddd, $J = 8.2, 2.3, 1.1$ Hz, 1H), 7.69 – 7.67 (m, 1H), 7.62 (s, 1H), 7.60 – 7.58 (m, 1H), 7.52 (t, $J = 7.9$ Hz, 1H), 7.28 – 7.25 (m, 1H), 7.20 (td, $J = 8.0, 7.5, 1.4$ Hz, 1H), 7.16 (td, $J = 7.4, 1.2$ Hz, 1H), 5.29 (s, 1H), 3.32 (dd, $J = 11.2, 6.3$ Hz, 1H), 3.21 – 3.16 (m, 1H), 3.00 – 2.94 (m, 1H), 2.89 – 2.84 (m, 1H), 1.95 (s, 1H). $^{13}\text{C NMR}$ (151 MHz, Chloroform-*d*) δ 148.51, 144.28, 136.07, 134.70, 132.70, 129.75, 127.25, 123.42, 123.21, 122.24, 119.73, 118.48, 110.99, 110.95, 57.19, 42.34, 22.39. **HRMS**: ESI calc. for $\text{C}_{17}\text{H}_{15}\text{N}_3\text{O}_2$ $[\text{M}+\text{H}]^+$: 294.1237, found 294.1235.

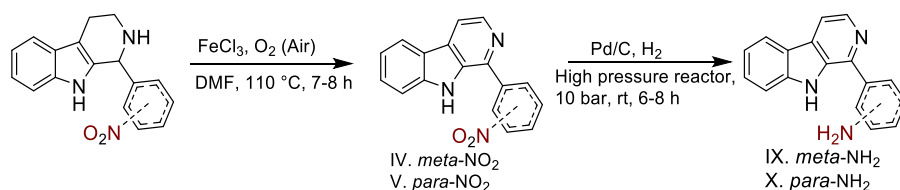
3.1.3. Synthesis of 1-(4-nitrophenyl)-2,3,4,9-tetrahydro-1H-pyrido[3,4-b]indole (II) —

Tryptamine and *para*-nitro benzaldehyde were used in the reaction following general protocol mentioned above. The crude reaction mixture was purified through column chromatography with a solvent gradient system of $\text{CH}_2\text{Cl}_2/\text{MeOH}$ (0-2%) to obtain a yellow solid compound with a 65% yield. Characterization: $^1\text{H NMR}$ (600 MHz, Chloroform-*d*) δ 8.21 (d, $J = 8.6$ Hz, 2H), 7.59 (d, $J = 7.7$ Hz, 1H), 7.56 (s, 1H), 7.53 (d, $J = 8.6$ Hz, 2H), 7.30 – 7.26 (m, 1H), 7.18 (dt, $J = 23.2, 7.3$ Hz, 2H), 5.30 (s, 1H), 3.35 – 3.29 (m, 1H), 3.22 – 3.16 (m, 1H), 2.99 – 2.93 (m, 1H), 2.88 (d, $J = 1.8$ Hz, 1H), 1.85 (s, 1H). $^{13}\text{C NMR}$ (151 MHz, Chloroform-*d*) δ 149.31, 147.74, 136.03, 132.65, 129.45, 127.20, 123.97, 122.29, 119.77, 118.47, 110.97, 110.89, 57.17, 42.29, 22.40. **HRMS**: ESI calc. for $\text{C}_{17}\text{H}_{15}\text{N}_3\text{O}_2$ $[\text{M}+\text{H}]^+$: 294.1237, found 294.1237.

3.1.4. Synthesis of 1-(2-nitrophenyl)-2,3,4,9-tetrahydro-1H-pyrido[3,4-b]indole (III) —

Tryptamine and *ortho*-nitro benzaldehyde were used in the reaction following general protocol mentioned above. The crude reaction mixture was purified through column chromatography with a solvent gradient system of $\text{CH}_2\text{Cl}_2/\text{MeOH}$ (0-2%) to obtain a yellow solid compound with a 56% yield. Characterization: $^1\text{H NMR}$ (600 MHz, Chloroform-*d*) δ 7.89 (dd, $J = 8.0, 1.5$ Hz, 2H), 7.59 (dd, $J = 7.4, 1.4$ Hz, 1H), 7.49 (td, $J = 7.5, 1.5$ Hz, 1H), 7.45 (td, $J = 7.7, 1.6$ Hz, 1H), 7.37 (dd, $J = 7.7, 1.6$ Hz, 1H), 7.26 – 7.23 (m, 1H), 7.18 (td, $J = 8.0, 7.5, 1.5$ Hz, 1H), 7.15 (td, $J = 7.4, 1.3$ Hz, 1H), 5.67 (s, 1H), 3.27 – 3.20 (m, 1H), 3.16 (ddd, $J = 12.1, 7.2, 4.7$ Hz, 1H), 2.96 (dddd, $J = 15.3, 6.9, 5.0, 1.6$ Hz, 1H), 2.89 – 2.82 (m, 1H), 2.18 (s, 2H). $^{13}\text{C NMR}$ (151 MHz, Chloroform-*d*) δ 149.96, 136.74, 136.02, 132.99, 132.53, 131.28, 128.71, 127.08, 124.22, 122.11, 119.58, 118.42, 111.31, 110.97, 52.17, 41.84, 22.28. **HRMS**: ESI calc. for $\text{C}_{17}\text{H}_{15}\text{N}_3\text{O}_2$ $[\text{M}+\text{H}]^+$: 294.1237, found 294.1237.

3.2. General method for the synthesis of β -carboline compounds (Aromatization) — To a mixture of tetrahydro- β -carboline (1 mmol) in DMF (5 mL), FeCl₃ (10 mol%, 16.2 mg) was added. The reaction was stirred at 110 °C. After the reaction (TLC control) was completed, the mixture was cooled to room temperature, and water was added. The reaction mixture was then extracted with EtOAc and washed with brine solution. The organic layer was dried over anhydrous Na₂SO₄ and concentrated under reduced pressure. The crude product was purified over silica gel in column chromatography (60-120 mesh size) using a gradient eluent of hexane/EtOAc (15-20%).²



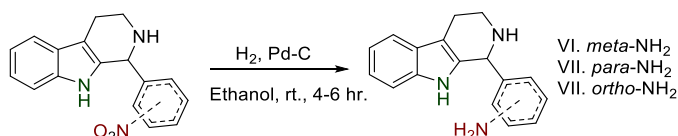
Scheme S2. Synthesis of the β -carboline compounds and their corresponding amine derivatives.

3.2.1. Synthesis of 1-(3-nitrophenyl)-9H-pyrido[3,4-b]indole (IV) — To a mixture of 1-(3-nitrophenyl)-2,3,4,9-tetrahydro-1H-pyrido[3,4-b]indole in DMF, FeCl₃ was added and the reaction was stirred at 110 °C, as mentioned in the above mentioned procedure. The crude reaction mixture was then extracted with EtOAc and purified over column chromatography to obtain a yellow solid with a 25% yield (Scheme S2). Characterization: ¹H NMR (600 MHz, DMSO-*d*₆) δ 11.73 (s, 1H), 8.81 (t, *J* = 2.0 Hz, 1H), 8.53 (d, *J* = 5.1 Hz, 1H), 8.49 (dt, *J* = 7.7, 1.4 Hz, 1H), 8.39 – 8.36 (m, 1H), 8.31 (d, *J* = 7.8 Hz, 1H), 8.23 (d, *J* = 5.1 Hz, 1H), 7.92 (t, *J* = 7.9 Hz, 1H), 7.67 – 7.65 (m, 1H), 7.60 (ddd, *J* = 8.2, 6.9, 1.2 Hz, 1H), 7.31 (ddd, *J* = 7.9, 6.9, 1.0 Hz, 1H). ¹³C NMR (151 MHz, DMSO-*d*₆) δ 149.10, 142.11, 140.68, 140.38, 139.54, 135.60, 134.07, 131.28, 130.71, 129.48, 124.01, 123.92, 122.70, 121.66, 120.71, 115.81, 113.24. HRMS: ESI calc. for C₁₇H₁₁N₃O₂ [M+H]⁺: 290.0924, found 290.0919.

3.2.2. Synthesis of 1-(4-nitrophenyl)-9H-pyrido[3,4-b]indole (V) — This compound has been synthesized from 1-(4-nitrophenyl)-2,3,4,9-tetrahydro-1H-pyrido[3,4-b]indole by following the same procedure to give a yellow solid with 30% yield (Scheme S2). Characterization: ¹H NMR (600 MHz, DMSO-*d*₆) δ 11.36 (s, 1H), 8.46 (dd, *J* = 5.1, 2.3 Hz, 1H), 8.34 (dd, *J* = 8.8, 1.9 Hz, 2H), 8.25 (dd, *J* = 8.9, 2.2 Hz, 2H), 8.11 (d, *J* = 7.8 Hz, 1H), 7.98 (d, *J* = 5.1 Hz, 1H), 7.59 (d, *J* = 8.2 Hz, 1H), 7.49 (dd, *J* = 8.7, 7.0 Hz, 1H), 7.22 (td, *J* = 7.5, 1.8 Hz, 1H). ¹³C NMR (151 MHz, DMSO-*d*₆) δ 147.60, 145.06, 141.71, 139.94, 139.20, 133.87, 130.37, 130.07,

129.09, 124.32, 122.28, 121.16, 120.33, 115.67, 112.87. **HRMS**: ESI calc. for C₁₇ H₁₁ N₃ O₂ [M+H]⁺: 290.0924, found 290.0919.

3.3. General method for reduction of nitro to the amine of tetrahydro β-carboline — The tetrahydro β-carboline derivatives and palladium in charcoal were charged in a two-neck round bottom flask. In proper dry condition, ethanol was added and stirred in the presence of hydrogen gas at room temperature for 6-8 hours. The reaction mixture was passed through celite, and ethanol was evaporated. The reaction mixture was then purified over column chromatography to get the pure amine.



Scheme S3. Synthesis of the amine derivatives of tetrahydro-β-carboline compounds.

3.3.1. Synthesis of 3-(2,3,4,9-tetrahydro-1H-pyrido[3,4-b]indol-1-yl)aniline (VI) — 1-(3-nitrophenyl)-2,3,4,9-tetrahydro-1H-pyrido[3,4-b]indole (300mg, 1.14 mmol) and palladium in charcoal (0.1 mmol) were used in the reaction following general procedure mentioned above and purified over column chromatography using a gradient eluent of EtOAc-hexane (35-40%) to get the pure product with 50% yield (Scheme S3). Characterization: ¹H NMR (600 MHz, Chloroform-*d*) δ 7.80 (s, 1H), 7.57 – 7.54 (m, 1H), 7.16 (d, *J* = 7.6 Hz, 1H), 7.15 – 7.14 (m, 2H), 7.13 – 7.12 (m, 1H), 6.73 (d, *J* = 7.5 Hz, 1H), 6.64 (dd, *J* = 8.1, 2.4 Hz, 1H), 6.53 (t, *J* = 2.0 Hz, 1H), 5.06 (s, 1H), 3.41 – 3.35 (m, 1H), 3.15 – 3.09 (m, 1H), 2.93 – 2.90 (m, 1H), 2.86 – 2.79 (m, 1H), 2.07 (s, 1H), 1.95 (s, 1H). ¹³C NMR (151 MHz, Chloroform-*d*) δ 146.88, 142.95, 135.83, 134.61, 129.75, 127.36, 121.65, 119.36, 118.77, 118.19, 114.92, 114.80, 110.90, 109.95, 58.08, 42.92, 22.49. **HRMS**: ESI calc. for C₁₇ H₁₇ N₃ [M+H]⁺: 264.1495, found 260.1495.

3.3.2. Synthesis of 4-(2,3,4,9-tetrahydro-1H-pyrido[3,4-b]indol-1-yl)aniline (VII) — 1-(4-nitrophenyl)-2,3,4,9-tetrahydro-1H-pyrido[3,4-b]indole was converted to the corresponding amine using the above-mentioned procedure. Purification was done using column chromatography using a gradient eluent of EtOAc-hexane (40%) to get the pure product with a 55% yield (Scheme S3). Characterization: ¹H NMR (600 MHz, Chloroform-*d*) δ 7.68 (s, 1H), 7.57 – 7.53 (m, 1H), 7.24 – 7.21 (m, 1H), 7.15 (d, *J* = 1.5 Hz, 1H), 7.14 – 7.12 (m, 1H), 7.10 (d, *J* = 8.3 Hz, 2H), 6.66 (d, *J* = 8.3 Hz, 2H), 3.42 – 3.36 (m, 1H), 3.14 (dd, *J* = 6.5, 2.9 Hz,

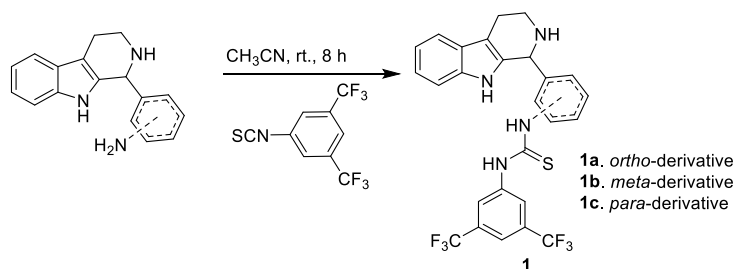
1H), 2.95 – 2.90 (m, 1H), 2.85 – 2.80 (m, 1H), 2.07 (broad s, 1H), 1.28 (s, 1H). ¹³C NMR (151 MHz, Chloroform-*d*) δ 146.40, 135.80, 135.05, 131.47, 129.60, 127.46, 121.59, 119.31, 118.18, 115.21, 110.82, 109.98, 57.57, 42.93, 22.49. **HRMS**: ESI calc. for C₁₇ H₁₇ N₃ [M+H]⁺: 264.1495, found 260.1498.

3.3.3. Synthesis of 2-(2,3,4,9-tetrahydro-1H-pyrido[3,4-*b*]indol-1-yl)aniline (VIII) — 1-(2-nitrophenyl)-2,3,4,9-tetrahydro-1H-pyrido[3,4-*b*]indole was converted to the corresponding amine using the same procedure. The amine was purified over silica gel (60-120 mesh size) in column chromatography, and the yield was 40% (Scheme S3). Characterization: ¹H NMR (600 MHz, Chloroform-*d*) δ 7.66 (s, 1H), 7.57 – 7.53 (m, 1H), 7.21 – 7.19 (m, 1H), 7.18 (dd, *J* = 7.6, 1.6 Hz, 1H), 7.15 (dd, *J* = 5.3, 1.6 Hz, 1H), 7.14 – 7.11 (m, 1H), 6.74 (td, *J* = 7.4, 1.2 Hz, 1H), 6.67 (dd, *J* = 7.9, 1.2 Hz, 1H), 5.22 (s, 1H), 3.41 – 3.35 (m, 1H), 3.17 – 3.12 (m, 1H), 2.96 – 2.92 (m, 1H), 2.86 – 2.81 (m, 1H), 2.08 (s, 1H). ¹³C NMR (151 MHz, Chloroform-*d*) δ 146.61, 135.74, 133.77, 130.07, 129.16, 127.41, 124.52, 121.63, 119.38, 118.13, 117.69, 116.66, 110.98, 109.71, 43.24, 22.47. **HRMS**: ESI calc. for C₁₇ H₁₇ N₃ [M+H]⁺: 264.1495, found 260.1498.

3.4. Synthesis of 3-(9H-pyrido[3,4-*b*]indol-1-yl)aniline (IX) — A mixture of 1-(3-nitrophenyl)-9H-pyrido[3,4-*b*]indole (100 mg, 0.346 mmol), 10% Pd/C(20 mg) and acetic acid (5 ml) was hydrogenated on a high-pressure reactor (Parr apparatus) at 10 bar pressure for 8 hours. The reaction mixture was neutralized by saturated Na₂CO₃ solution and extracted with ethyl acetate. Then, it was filtered through celite and the organic layer was dried over sodium sulfate and evaporated to get the pure amine (yield- 70%) (Scheme S2). Characterization: ¹H NMR (600 MHz, Chloroform-*d*) δ 8.61 (s, 1H), 8.57 (d, *J* = 5.2 Hz, 1H), 8.18 (d, *J* = 7.9 Hz, 1H), 7.95 (d, *J* = 5.2 Hz, 1H), 7.62 – 7.55 (m, 1H), 7.53 (d, *J* = 8.1 Hz, 1H), 7.39 (t, *J* = 7.6 Hz, 1H), 7.36 (dt, *J* = 9.0, 1.3 Hz, 1H), 7.34 – 7.32 (m, 1H), 7.31 (t, *J* = 1.9 Hz, 1H), 6.84 (dd, *J* = 7.7, 1.3 Hz, 1H), 1.65 (s, 2H). ¹³C NMR (151 MHz, Chloroform-*d*) δ 147.23, 143.18, 140.47, 139.39, 139.01, 133.55, 129.97, 129.72, 128.44, 121.75, 121.65, 120.09, 118.20, 115.65, 114.94, 113.79, 111.65. **HRMS**: ESI calc. for C₁₇ H₁₃ N₃ [M+H]⁺: 260.1182, found 260.1185.

3.5. Synthesis of 4-(9H-pyrido[3,4-*b*]indol-1-yl)aniline (X) — A mixture of 1-(4-nitrophenyl)-9H-pyrido[3,4-*b*]indole (100 mg, 0.346 mmol), 10% Pd/C(20 mg) and acetic acid (5 ml) was hydrogenated on a high-pressure reactor (Parr apparatus) at 10 bar pressure for 8 hours. The

reaction mixture was neutralized by saturated Na_2CO_3 solution and extracted with ethyl acetate. Then, it was filtered through celite and the organic layer was dried over sodium sulfate and evaporated to get the pure amine (yield- 75%) (Scheme S2). Characterization: $^1\text{H NMR}$ (600 MHz, Chloroform-*d*) δ 8.66 (s, 1H), 8.52 (d, $J = 5.3$ Hz, 1H), 8.16 (d, $J = 7.9$ Hz, 1H), 7.89 (d, $J = 5.3$ Hz, 1H), 7.79 (d, $J = 8.0$ Hz, 2H), 7.56 (t, $J = 7.6$ Hz, 1H), 7.52 (d, $J = 8.1$ Hz, 1H), 7.31 (t, $J = 7.4$ Hz, 1H), 6.87 (d, $J = 7.9$ Hz, 2H), 2.28 (s, 2H). $^{13}\text{C NMR}$ (151 MHz, Chloroform-*d*) δ 153.01, 148.42, 146.03, 143.05, 137.98, 134.36, 133.95, 132.63, 132.43, 126.15, 126.04, 124.20, 119.57, 117.32, 117.23. **HRMS**: ESI calc. for $\text{C}_{17}\text{H}_{13}\text{N}_3$ $[\text{M}+\text{H}]^+$: 260.1182, found 260.1186.

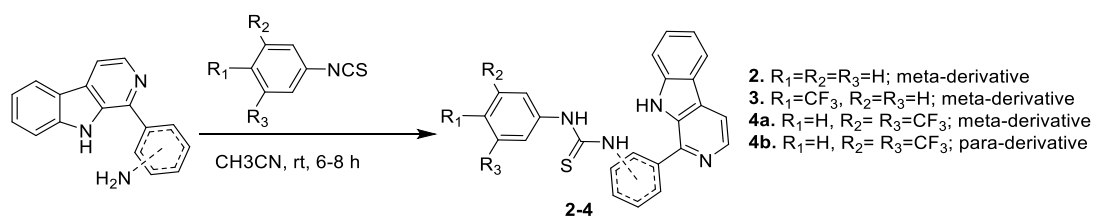


Scheme S4. Synthesis of the thiourea derivatives of amine derivatives of tetrahydro- β -carboline compounds.

3.6. Synthesis of 1-(3,5-bis(trifluoromethyl)phenyl)-3-(2-(2,3,4,9-tetrahydro-1H-pyrido[3,4-b]indol-1-yl)phenyl)thiourea (1a) — To the stirring solution of 2-(2,3,4,9-tetrahydro-1H-pyrido[3,4-b]indol-1-yl)aniline (50 mg, 0.19 mmol) in acetonitrile, 1-isothiocyanato-3,5-bis(trifluoromethyl)benzene (56.64 mg, 0.209 mmol) was added and stirred at room temperature for 6 hours. Then, the solvent was evaporated, and the crude mixture was purified over silica gel (60-120 mesh) in column chromatography using 30% EtOAc-hexane as eluent to get the pure product with a yield of 60% (Scheme S4). Characterization: $^1\text{H NMR}$ (600 MHz, DMSO-*d*₆) δ 11.08 (s, 1H), 10.04 (s, 1H), 8.09 (s, 2H), 7.87 (s, 1H), 7.75 (s, 1H), 7.50 (d, $J = 7.8$ Hz, 1H), 7.29 (d, $J = 8.1$ Hz, 1H), 7.10 (t, $J = 7.6$ Hz, 1H), 7.07 – 7.04 (m, 1H), 7.03 (d, $J = 7.5$ Hz, 1H), 6.72 (d, $J = 8.0$ Hz, 1H), 6.45 (d, $J = 5.3$ Hz, 2H), 5.81 (s, 2H), 4.52 (s, 1H), 3.51 (s, 1H), 3.23 – 3.16 (m, 1H), 2.86 (td, $J = 18.3, 16.4, 2.6$ Hz, 1H), 2.53 – 2.46 (m, 1H). $^{13}\text{C NMR}$ (151 MHz, DMSO-*d*₆) δ 180.87, 147.51, 143.15, 136.70, 132.76, 130.80, 130.58, 130.36, 130.14, 129.93, 129.58, 126.80, 126.58, 124.61, 122.80, 121.75, 119.13, 118.31, 111.69, 109.07, 57.75, 41.61, 21.53. **HRMS**: ESI calc. for $\text{C}_{26}\text{H}_{20}\text{F}_6\text{N}_4\text{S}$ $[\text{M}+\text{H}]^+$: 535.1386, found 535.1391.

3.7. Synthesis of 1-(3,5-bis(trifluoromethyl)phenyl)-3-(3-(2,3,4,9-tetrahydro-1H-pyrido[3,4-b]indol-1-yl)phenyl)thiourea (1b) — To the stirring solution of 3-(2,3,4,9-tetrahydro-1H-pyrido[3,4-b]indol-1-yl)aniline in acetonitrile, 1-isothiocyanato-3,5-bis(trifluoromethyl)benzene was added and stirred at room temperature. The progress of the reaction was monitored by TLC (50% EtOAc-hexane). Then, the solvent was evaporated, and the crude mixture was purified over silica gel (60-120 mesh) in column chromatography using 40-45% EtOAc-hexane as eluent to get the pure product with a yield of 65% (Scheme S4). Characterization: $^1\text{H NMR}$ (600 MHz, DMSO- d_6) δ 11.16 (s, 1H), 9.92 (s, 1H), 8.14 (s, 2H), 7.83 (s, 1H), 7.50 (d, $J = 7.8$ Hz, 1H), 7.33 (d, $J = 8.1$ Hz, 1H), 7.11 (t, $J = 7.6$ Hz, 1H), 7.02 (q, $J = 7.5$ Hz, 2H), 6.63 (d, $J = 7.8$ Hz, 1H), 6.60 (s, 1H), 6.53 (dd, $J = 8.0, 2.3$ Hz, 1H), 5.17 (s, 1H), 4.61 (s, 1H), 3.47 (td, $J = 13.4, 4.1$ Hz, 1H), 3.13 (m, 1H), 2.84 (dd, $J = 15.5, 4.1$ Hz, 1H), 2.51 (m, 1H). $^{13}\text{C NMR}$ (151 MHz, DMSO- d_6) δ 181.00, 149.26, 143.59, 140.75, 136.71, 130.21, 129.99, 129.36, 126.62, 126.29, 124.68, 122.87, 121.67, 119.09, 118.32, 115.96, 113.94, 113.79, 111.70, 108.58, 59.11, 41.99, 21.80. **HRMS**: ESI calc. for $\text{C}_{26}\text{H}_{20}\text{F}_6\text{N}_4\text{S}$ [$\text{M}+\text{H}$] $^+$: 535.1386, found 535.1390.

3.8. Synthesis of 1-(3,5-bis(trifluoromethyl)phenyl)-3-(4-(2,3,4,9-tetrahydro-1H-pyrido[3,4-b]indol-1-yl)phenyl)thiourea (1c) — To the stirring solution of 4-(2,3,4,9-tetrahydro-1H-pyrido[3,4-b]indol-1-yl)aniline, 1-isothiocyanato-3,5-bis(trifluoromethyl)benzene was added and stirred at room temperature. The progress of the reaction was monitored by TLC (50% EtOAc-hexane). Then, the solvent was evaporated, and the crude mixture was purified through column chromatography using 40% EtOAc-hexane as eluent to get the pure product yielding 70% (Scheme S4). Characterization: $^1\text{H NMR}$ (600 MHz, DMSO- d_6) δ 11.07 (s, 1H), 10.97 (s, 1H), 10.85 (s, 0H), 8.36 (s, 2H), 7.83 (s, 1H), 7.70 (d, $J = 8.1$ Hz, 2H), 7.55 (d, $J = 7.9$ Hz, 1H), 7.39 (d, $J = 8.1$ Hz, 2H), 7.31 (d, $J = 8.2$ Hz, 1H), 7.13 (t, $J = 7.6$ Hz, 1H), 7.06 (t, $J = 7.5$ Hz, 1H), 5.94 (s, 1H), 3.44 (d, $J = 5.3$ Hz, 1H), 3.12 (q, $J = 7.9, 6.1$ Hz, 2H), 3.04 (dd, $J = 13.6, 7.8$ Hz, 2H). $^{13}\text{C NMR}$ (151 MHz, DMSO- d_6) δ 180.09, 142.11, 140.82, 137.00, 131.18, 130.76, 130.67, 130.54, 128.81, 126.13, 124.59, 124.08, 122.93, 122.50, 119.50, 118.70, 112.04, 107.85, 55.56, 40.48, 18.62. **HRMS**: ESI calc. for $\text{C}_{26}\text{H}_{20}\text{F}_6\text{N}_4\text{S}$ [$\text{M}+\text{H}$] $^+$: 535.1386, found 535.1390.



Scheme S5. Synthesis of the thiourea derivatives of amine derivatives of β -carboline compounds.

3.9. Synthesis of 1-(3-(9H-pyrido[3,4-b]indol-1-yl)phenyl)-3-phenylthiourea (2) — To the stirring solution of 3-(9H-pyrido[3,4-b]indol-1-yl)aniline, isothiocyanatobenzene was added and stirred at room temperature till the completion of the reaction, monitored by TLC (40% EtOAc-hexane). Then, the solvent was evaporated, and the crude mixture was purified through column chromatography using 35% EtOAc-hexane as eluent to get the pure product yielding 70% (Scheme S5). Characterization: 1H NMR (600 MHz, DMSO- d_6) δ 11.51 (s, 1H), 10.03 (s, 1H), 9.99 (s, 1H), 8.47 (d, $J = 5.2$ Hz, 1H), 8.28 (d, $J = 7.9$ Hz, 1H), 8.14 (d, $J = 5.0$ Hz, 1H), 8.11 (s, 1H), 7.79 (d, $J = 7.7$ Hz, 1H), 7.75 (d, $J = 8.1$ Hz, 1H), 7.63 (d, $J = 8.3$ Hz, 1H), 7.58 (d, $J = 8.6$ Hz, 1H), 7.56 (d, $J = 8.3$ Hz, 1H), 7.53 (d, $J = 8.0$ Hz, 2H), 7.36 (t, $J = 7.9$ Hz, 2H), 7.28 (t, $J = 7.7$ Hz, 1H), 7.15 (t, $J = 7.6$ Hz, 1H). ^{13}C NMR (151 MHz, DMSO- d_6) δ 180.04, 142.26, 141.47, 140.33, 139.87, 139.03, 138.87, 133.48, 129.68, 129.26, 128.98, 128.72, 125.05, 124.70, 124.31, 123.97, 123.76, 122.15, 121.30, 120.05, 114.52, 112.78. HRMS: ESI calc. for $C_{24}H_{18}N_4S$ [$M+H$] $^+$: 395.1325, found 395.1324.

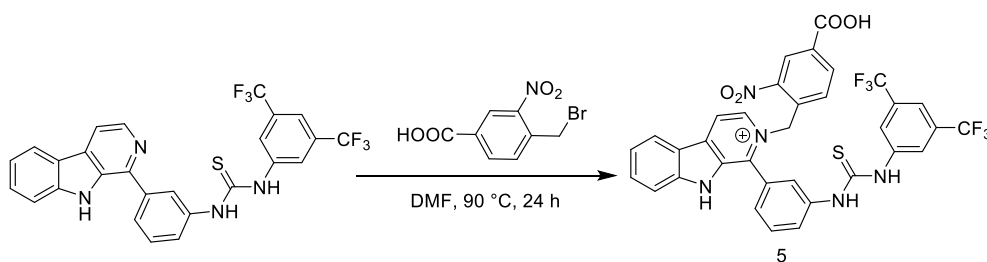
3.10. Synthesis of 1-(3-(9H-pyrido[3,4-b]indol-1-yl)phenyl)-3-(4-(trifluoromethyl)phenyl)thiourea (3) — To the stirring solution of 3-(9H-pyrido[3,4-b]indol-1-yl)aniline, 1-isothiocyanato-4-(trifluoromethyl)benzene was added and stirred at room temperature till the completion of the reaction, monitored by TLC (40%EtOAc-hexane). Then, the solvent was evaporated, and the crude mixture was purified through column chromatography using 35% EtOAc-hexane as eluent to get the pure product with a yield of 70% (Scheme S5). Characterization: 1H NMR (600 MHz, DMSO- d_6) δ 11.51 (s, 1H), 10.28 (s, 2H), 8.47 (dd, $J = 5.2, 1.8$ Hz, 1H), 8.28 (d, $J = 7.8$ Hz, 1H), 8.15 (d, $J = 5.1$ Hz, 1H), 8.12 (s, 1H), 7.83 (d, $J = 7.7$ Hz, 1H), 7.80 (d, $J = 8.4$ Hz, 2H), 7.76 (d, $J = 8.2$ Hz, 1H), 7.71 (d, $J = 8.3$ Hz, 2H), 7.63 (t, $J = 6.0$ Hz, 1H), 7.60 (d, $J = 8.6$ Hz, 1H), 7.56 (t, $J = 7.6$ Hz, 1H), 7.28 (t, $J = 7.5$ Hz, 1H). ^{13}C NMR (151 MHz, Chloroform- d) δ 184.82, 148.59, 146.91, 146.23, 144.81, 143.92, 143.64, 138.23, 134.48, 134.12, 133.49, 130.88, 130.85, 130.51, 129.79,

128.83, 128.60, 128.27, 126.90, 126.05, 124.82, 119.31, 117.53. **HRMS**: ESI calc. for $C_{25}H_{17}F_3N_4S$ $[M+H]^+$: 463.1199, found 463.1197.

3.11. Synthesis of 1-(3-(9H-pyrido[3,4-b]indol-1-yl)phenyl)-3-(3,5-bis(trifluoromethyl)phenyl)thiourea (4a) — To the stirring solution of 3-(9H-pyrido[3,4-b]indol-1-yl)aniline, 1-isothiocyanato-3,5-bis(trifluoromethyl)benzene was added and stirred at room temperature till the completion of the reaction, monitored by TLC (40%EtOAc-hexane). Then, the solvent was evaporated, and the crude mixture was purified over silica gel (100-200 mesh size) through column chromatography using 35% EtOAc-hexane as eluent to get the pure product with a yield of 50% (Scheme S5). Characterization: 1H NMR (400 MHz, DMSO- d_6) δ 11.49 (s, 1H), 10.47 (s, 1H), 10.38 (s, 1H), 8.46 (d, $J = 5.1$ Hz, 1H), 8.28 (d, $J = 1.9$ Hz, 2H), 8.26 (s, 1H), 8.14 (d, $J = 5.1$ Hz, 1H), 8.08 (t, $J = 2.0$ Hz, 1H), 7.86 (d, $J = 7.8$ Hz, 1H), 7.81 (s, 1H), 7.70 (d, $J = 8.4$ Hz, 1H), 7.62 (dd, $J = 8.1, 5.8$ Hz, 2H), 7.58 – 7.52 (m, 1H), 7.27 (t, $J = 7.4$ Hz, 1H). ^{13}C NMR (151 MHz, DMSO- d_6) δ 180.34, 142.30, 142.00, 141.49, 139.57, 139.37, 138.88, 133.46, 130.40, 129.77, 129.60, 128.74, 125.44, 124.63, 124.41, 124.21, 124.00, 122.16, 122.16, 121.28, 120.08, 114.61, 112.72. **HRMS**: ESI calc. for $C_{26}H_{16}F_6N_4S$ $[M+H]^+$: 531.1073, found 531.1071.

3.12. Synthesis of 1-(4-(9H-pyrido[3,4-b]indol-1-yl)phenyl)-3-(3,5-bis(trifluoromethyl)phenyl)thiourea (4b) — To the stirring solution of 4-(9H-pyrido[3,4-b]indol-1-yl)aniline, 1-isothiocyanato-3,5-bis(trifluoromethyl)benzene was added and stirred at room temperature till the completion of the reaction, monitored by TLC (40% EtOAc-hexane). Then, the solvent was evaporated, and the crude mixture was purified over silica gel (100-200 mesh size) through column chromatography using 35% EtOAc-hexane as eluent to get the pure product with a yield of 50%. Characterization: 1H NMR (600 MHz, DMSO- d_6) δ 11.60 (s, 1H), 10.55 (s, 1H), 10.41 (s, 1H), 8.47 (d, $J = 5.1$ Hz, 1H), 8.32 (s, 2H), 8.28 (d, $J = 7.9$ Hz, 1H), 8.14 (d, $J = 5.2$ Hz, 1H), 8.08 (d, $J = 8.5$ Hz, 2H), 7.84 (s, 1H), 7.75 (d, $J = 8.5$ Hz, 2H), 7.68 (d, $J = 8.2$ Hz, 1H), 7.57 (ddd, $J = 8.2, 7.0, 1.2$ Hz, 1H), 7.30 – 7.26 (m, 1H). ^{13}C NMR (151 MHz, DMSO- d_6) δ 180.23, 142.31, 133.30, 130.66, 130.44, 129.23, 128.75, 124.64, 124.17, 123.95, 123.94, 123.92, 122.83, 122.11, 121.25, 120.06, 117.44, 114.32, 112.93. **HRMS**: ESI calc. for $C_{26}H_{16}F_6N_4S$ $[M+H]^+$: 531.1073, found 531.1077.

3.13. Synthesis of 1-(3-(3-(3,5-bis(trifluoromethyl)phenyl)thioureido)phenyl)-2-(4-carboxy-2-nitrobenzyl)-9H-pyrido[3,4-b]indol-2-ium (5) — To the stirring solution of compound **4a** (30 mg, 0.0422 mmol) in DMF, 4-(bromomethyl)-3-nitrobenzoic acid (12.07 mg, 0.0464 mmol) in DMF was added dropwise and stirred the mixture in 90 °C for 24 hours. Then, the reaction mixture was cooled down to room temperature and purified through column chromatography to get the desired pure product with 40% yield (Scheme S6). Characterization: $^1\text{H NMR}$ (600 MHz, DMSO- d_6) δ 11.68 (s, 1H), 10.51 (s, 1H), 10.43 (s, 1H), 8.49 (d, $J = 5.5$ Hz, 1H), 8.48 (s, 1H), 8.32 (d, $J = 7.8$ Hz, 1H), 8.29 (s, 2H), 8.24 (d, $J = 7.9$ Hz, 2H), 8.09 (s, 1H), 7.90 (d, $J = 8.0$ Hz, 1H), 7.86 (d, $J = 7.7$ Hz, 1H), 7.83 (s, 1H), 7.74 (d, $J = 8.3$ Hz, 1H), 7.64 (dd, $J = 13.6, 7.8$ Hz, 2H), 7.60 (d, $J = 7.5$ Hz, 1H), 7.30 (t, $J = 7.5$ Hz, 1H), 4.98 (s, 2H). $^{13}\text{C NMR}$ (151 MHz, DMSO- d_6) δ 180.40, 165.62, 159.33, 148.31, 142.15, 137.15, 134.62, 134.42, 134.32, 133.81, 133.32, 133.31, 132.83, 130.91, 130.89, 130.68, 130.46, 130.01, 129.29, 128.77, 126.26, 125.45, 124.60, 124.14, 122.79, 117.67, 115.91, 113.11, 111.54, 60.43. **HRMS:** ESI calc. for $\text{C}_{34}\text{H}_{22}\text{F}_6\text{N}_5\text{O}_4\text{S}$ [**M**]: 710.1297, found 710.1297.



Scheme S6. Synthesis of the Photo cleavable proanionophore compound.

4. Determination of pK_a Values Using UV-Vis Spectrophotometer:

The pK_a values of compounds in aqueous solution were measured by monitoring the changes in absorbance of the compounds at different pH.³ The UV-Vis spectra of the compounds were recorded in a Perkin-Elmer Lambda 25 UV-Visible spectrophotometer, and the pH measurements were performed using a HI 2210 pH meter (HANNA Instruments) at 298 K. Different buffer solutions were prepared by adding 1:1 K_2HPO_4 and KH_2PO_4 buffer solutions and the pH were adjusted to acidic and basic by adding 1 M HCl and 1 M NaOH solutions respectively. The pH of the solutions was varied from 4 to 11. The stock solutions of compounds were prepared in DMSO (10 mM) and appropriately diluted using buffer solutions of different pH to obtain a 0.03 mM solution of the compounds. The absorbance values at the wavelength (nm) at which the maximum changes were observed were plotted against the pH

values. The pK_a values were determined from the sigmoidal curves obtained from the plot of absorbance vs. pH.

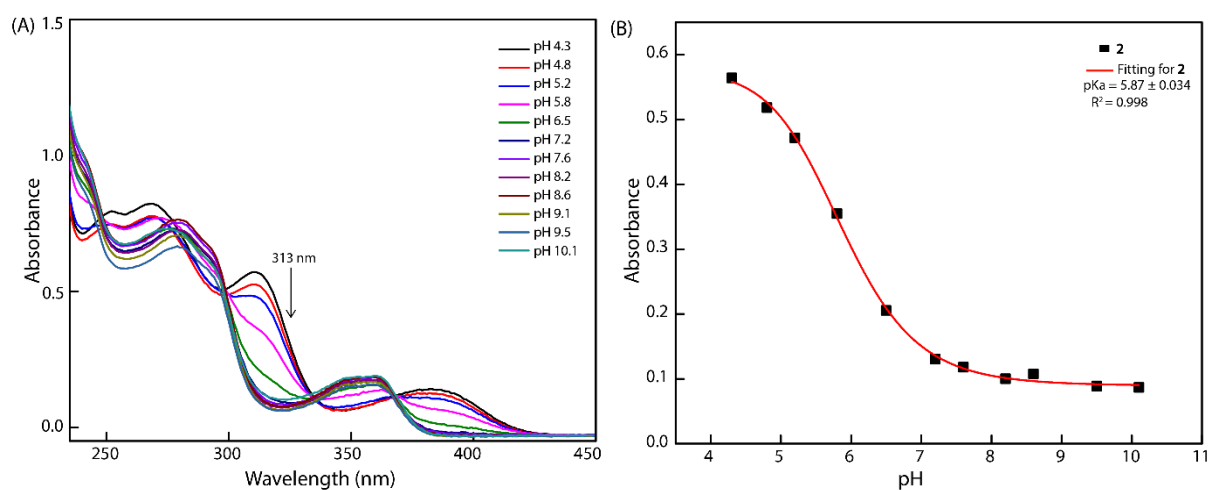


Fig. S1. Absorbance spectra of compound **2** (0.03 mM) at different pH buffer solutions (A). Comparison plots of absorbance at 313 nm at different pH (B).

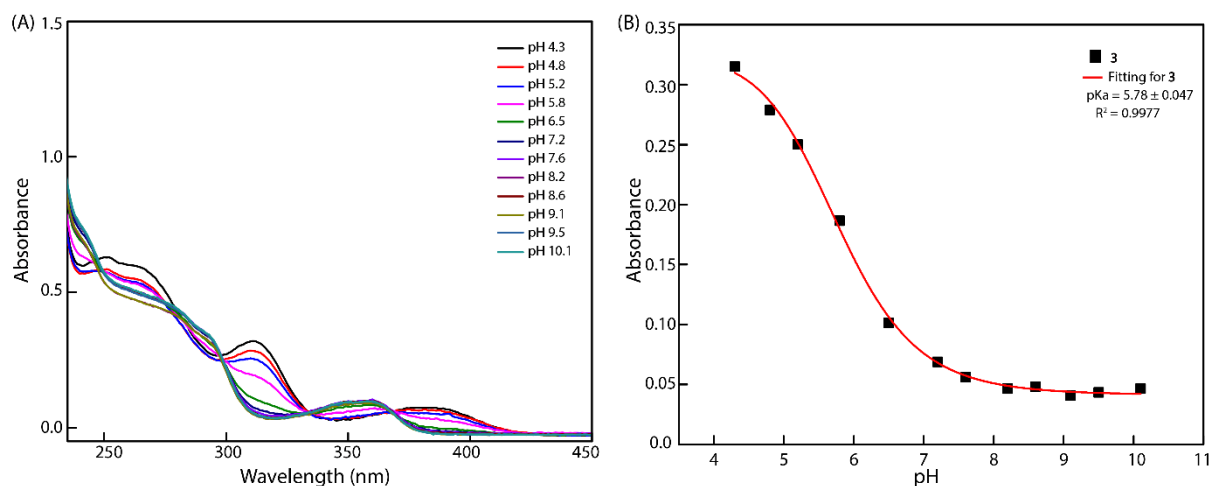


Fig. S2. Absorbance spectra of compound **3** (0.03 mM) at different pH buffer solutions (A). Comparison plots of absorbance at 313 nm at different pH (B).

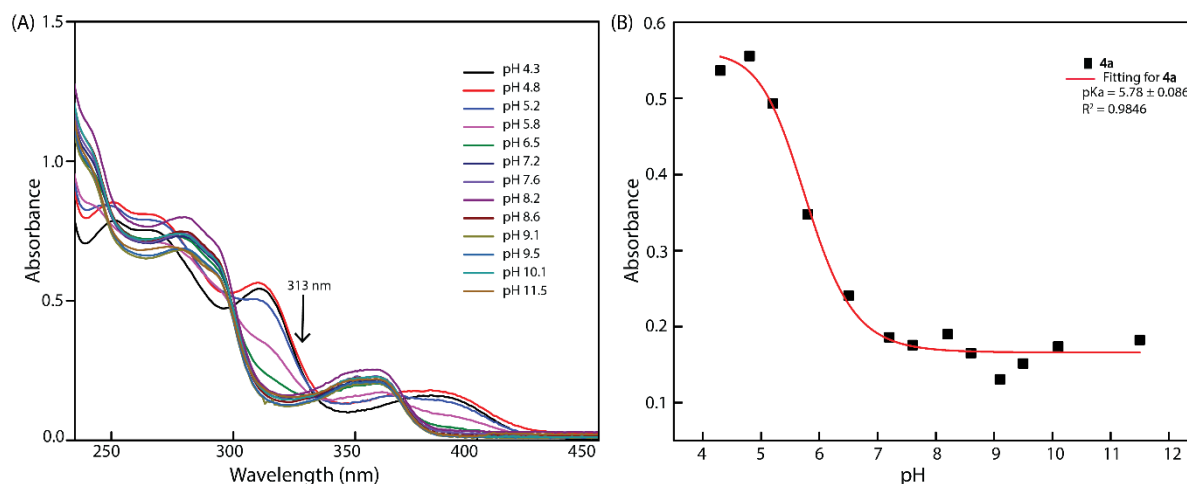


Fig. S3. Absorbance spectra of compound **4a** (0.03 mM) at different pH buffer solutions (A). Comparison plots of absorbance at 313 nm at different pH (B).

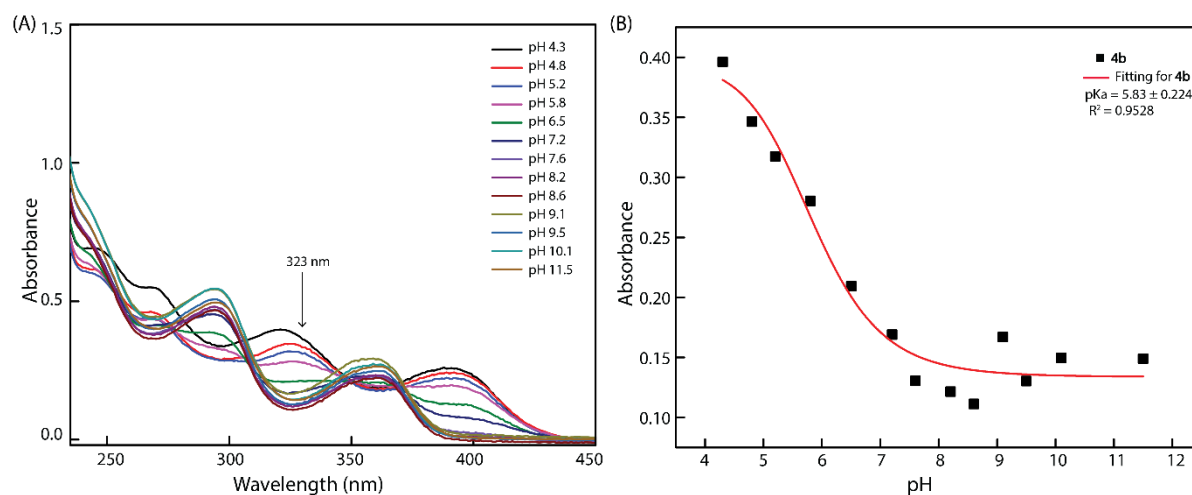


Fig. S4. Absorbance spectra of compound **4b** (0.03 mM) at different pH buffer solutions (A). Comparison plots of absorbance at 323 nm at different pH (B).

5. Ion Transport Studies:

5.1. Ion transport studies with the fluorescence-based assay

5.1.1. buffer and stock solution preparation — The required buffer solution was prepared by dissolving HEPES and salt (LiCl, NaCl, KCl, RbCl, CsCl, and NaCl, NaBr, NaI, NaNO₃) in Milli-Q water to obtain a buffer composition of 20 mM HEPES buffer, pH 7.2, containing 100 mM of the respective salt (MCl or Na_xA). The stock solutions of the compounds were prepared in molecular biology grade DMSO solvent. The concentration of DMSO stock solution used for our experiment is 0.26% for both ionophore and pro-anionophore.

5.1.2. Preparation of EYPC/CHOL-LUVs \supset lucigenin — For conducting the lucigenin-based ion transport studies,⁴ egg yolk phosphatidylcholine (EYPC, 50 mg/mL in deacidified CHCl_3) and CHOL (25 mg/mL in deacidified CHCl_3) was taken in a clean sample vial in the molar ratio of 8:2. The solution was evaporated by continuous rotation for 6 h under reduced pressure to form a thin lipid film. The thin lipid film was rehydrated by adding 800 μL of 20 mM HEPES buffer containing 1 mM lucigenin and 100 mM NaNO_3 solution, pH 7.2. The resultant suspension was vortexed 6-7 times for 1 h, followed by 17-19 freeze-thaw cycles and, finally, 15 minutes of constant vortexing to incorporate lucigenin within the lipid bilayer. The lipid suspension was extruded using a mini extruder (a polycarbonate membrane from Avanti Polar Lipids) with a 200 nm pore size 19-21 times (must be an odd number). The unencapsulated lucigenin dye was removed by size exclusion column chromatography (Sephadex G-50) and 20 mM HEPES buffer containing 100 mM NaNO_3 solution, pH 7.2 as the eluting solution to get the final lipid concentration of 25 mM (assuming 100% lipid regeneration).

5.1.3. Quantitative measurement of transport activity from lucigenin assay — The fluorescence emission intensities of the lucigenin dye were normalized, and the intensities appearing at $t = 0$ and $t = 500$ s were taken as 0 and 100 units, respectively. The normalized fluorescent intensities (FI) at $t = 450$ s (before the addition of Triton X-100 solution) were considered to measure the transport activity of the compounds.

i.e. Transport activity,

$$T_{HPTS} = \frac{F_t - F_0}{F_\infty - F_0} \times 100\% \quad \dots\dots\dots \text{(Eq. S1)}$$

Where,

F_t = fluorescence intensity at $t = 450$ s (before the addition of Triton X-100 solution), F_0 = fluorescence intensity immediately before the addition of the transporter ($t = 0$ s), and F_∞ = fluorescence intensity after the addition of Triton X-100 solution (*i.e.*, at saturation after complete leakage at $t = 500$ s).

5.2. Ion transport activity studies using ion-selective electrode (ISE)-based assay:

5.2.1. Chloride ion efflux studies using chloride ion-selective electrode (ISE) — The Cl^- ion transport activities of the compounds were measured by monitoring the Cl^- ion concentration outside the liposomes using a chloride ion-selective electrode (chloride-ISE) (Thermo Scientific™ Orion™).⁵ Before each experiment, the ISE was calibrated using 1 ppm, 10 ppm, and 100 ppm of standard chloride solution with an ionic strength adjuster solution. A filling

solution was poured inside the electrode up to the mark before each experimental session. Chloride concentration (ppm) appearing in the display of the ion meter was set in continuous mode for the time-dependent measurements.

5.2.2. Preparation of EYPC/CHOL-LUV — The LUVs were prepared according to the reported procedure using EYPC and CHOL, as mentioned in the earlier section. The dry film was hydrated with 800 μL of 5 mM Phosphate buffer and 100 mM NaCl. The unilamellar vesicles were dialyzed with 5 mM phosphate buffer, pH 7.2, containing 100 mM NaNO_3 to remove the extravesicular NaCl from the solution. Finally, the LUVs were collected, and the volume was adjusted to 800 μL using phosphate buffer (5 mM) and NaNO_3 (100 mM) solution. The final lipid concentration was 25 mM (assuming 100% lipid regeneration).

5.2.3. Chloride efflux study across EYPC/CHOL-LUV — To measure the extent of efflux of Cl^- in the absence and presence of the compound, the EYPC/CHOL-LUVs (50 μL) and 5 mM phosphate buffer, pH 7.2, containing 100 mM NaNO_3 (3940 μL) were taken in a clean and dry glass vial and kept under mild stirring condition. The glass electrode was immersed into the solution under mild stirring conditions. To initiate the Cl^- transport kinetics at $t = 50$ s, 10 μL of the respective compound (from DMSO stock solution) was added into the stirring solution, and the readings were noted from the ion meter. After 5 minutes, the vesicles were lysed using 50 μL of 20% Triton X-100 solution. The total Cl^- efflux reading was taken at 7 minutes (allowing complete disruption of the LUVs). The initial reading was considered 0% Cl^- efflux, and the final reading at 7 min was considered 100% Cl^- efflux.

5.2.5. Ion selectivity studies:

5.2.5.1. Cation Selectivity studies across EYPC/CHOL-LUV \Rightarrow lucigenin — The cation selectivity studies were performed according to the reported procedure⁶. (section 1.1.2). Briefly, in a clean fluorescence cuvette, 2940 μL of buffer solution (100 mM MCl, 20 mM HEPES, pH 7.2; where $\text{M}^+ = \text{Li}^+, \text{Na}^+, \text{K}^+, \text{Rb}^+, \text{and Cs}^+$), 50 μL of above-prepared vesicles solution were taken, and fluorescence cuvette was placed in a fluorescence instrument equipped with a magnetic stirrer at $t = 0$ s. The fluorescence emission intensity of the lucigenin dye was measured at $\lambda_{\text{em}} = 505$ nm (where $\lambda_{\text{ex}} = 455$ nm) for the time course of 0 to 500 s. At $t = 50$ s, between the intra- and extravesicular medium, which increases the fluorescence intensity. Triton X-100 (20 μL of 20% solution in water) was added at $t = 450$ s to destroy all the vesicles.

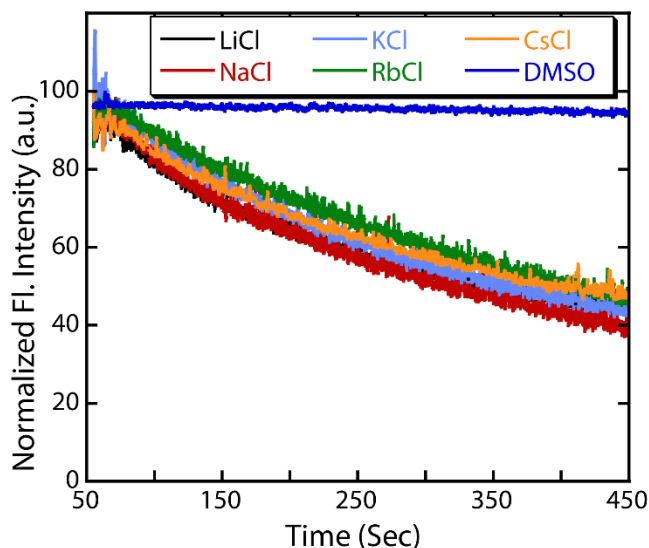


Fig. S5. Lucigenin-based cation transport selectivity studies of **4a** (10 μ M).

5.2.5.2. Anion selectivity studies across EYPC/CHOL-LUV Δ HPTS with pH Gradient — The anion selectivity studies were performed according to the reported procedure. Briefly, 2930 μ L of 20 mM HEPES buffer, containing 100 mM of the respective salt of NaX_y (where $\text{NaX}_y = \text{NaCl}, \text{NaBr}, \text{NaI}, \text{NaNO}_3$ and NaSCN) and 50 μ L of EYPC/CHOL-LUV Δ HPTS (prepared in 20 mM HEPES buffer containing 100 mM NaCl, pH 7.2) were taken in a fluorescence cuvette. Then 10 μ L of 1M NaOH was added to generate the pH gradient ($\Delta\text{pH}=0.8$). It was placed in the fluorescence spectrophotometer at room temperature under slow stirring conditions for equilibration. The HPTS fluorescence intensity of the solution was monitored. After 50 s, 10 μ L of the respective compound (from DMSO stock) was added to initiate the anion transport kinetics. At 450 s, the vesicles were lysed by adding 20 μ L of 20% Triton X-100 solution, and the fluorescence measurement was continued up to $t = 500$ s.

Note: The compound **4a** followed an anion transport efficacy with a sequence of $\text{Cl}^- > \text{I}^- > \text{SCN}^- > \text{Br}^- > \text{NO}_3^-$ as mentioned in Fig. 1b. To discuss the transport efficiency order mentioned in the manuscript, it is important to mention that, for a compound to be a good ion transporter the binding affinity should be optimal as the transport requires both swift association as well as dissociation with the ion. Association and dissociation should be in dynamic equilibrium. The enthalpy change between the hydration energy of the ions and the binding energy with the ionophore plays an important role. The thermodynamic enthalpy change (between hydration energy and binding energy of the anion) for chloride seems to be in an optimal range where the complexation and decomplexation process becomes a dynamic equilibrium which helps both

bindings of chloride inside hydrophobic lipid membrane and releases outside the membrane. Here, it is noteworthy to mention that the enthalpy change factor seems to be in favour of chloride as the thiourea moiety in the binding site has a selectively strong affinity towards chloride, which leads to the selectively better transport of chloride compared to other anions.⁷⁻⁹

5.2.5.3. Anion selectivity studies across EYPC/CHOL-LUV \Rightarrow HPTS without pH Gradient —

The anion selectivity studies were performed according to the reported procedure. Briefly, 2940 μ L of 20 mM HEPES buffer, pH 7.2, containing 100 mM of the respective salt of NaX_Y (where NaX_Y = NaCl, NaBr, NaI, NaNO₃, NaSCN and Na₂SO₄) and 50 μ L of EYPC/CHOL-LUV \Rightarrow HPTS (prepared in 20 mM HEPES buffer containing 100 mM NaCl, pH 7.2) were taken in a fluorescence cuvette. Then, it was placed in the fluorescence spectrophotometer at room temperature under slow stirring conditions. The HPTS fluorescence intensity of the solution was monitored. After 50 s, 10 μ L of the respective compound (from DMSO stock) was added to initiate the anion transport kinetics. At 450 s, the vesicles were lysed by adding 20 μ L of 20% Triton X-100 solution, and the fluorescence measurement was continued up to t = 500 s.

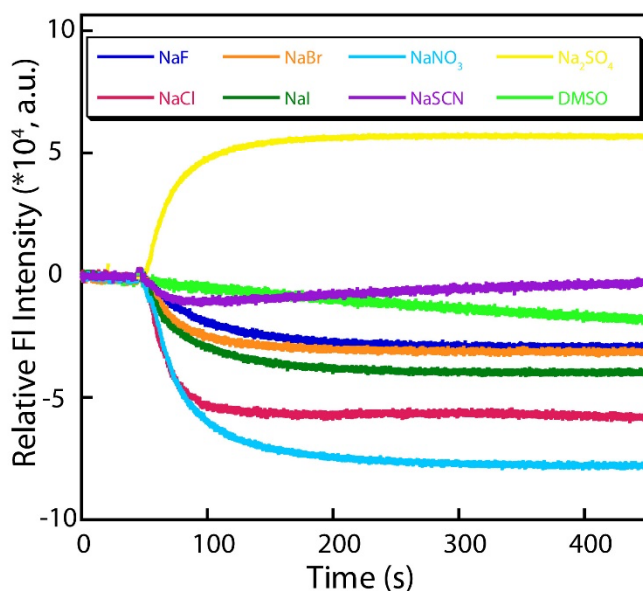


Fig. S6. Anion selectivity study **4a** using anion gradient assay across EYPC/CHOL-LUVs \Rightarrow HPTS where intravesicular solution contains 20 mM HEPES buffers, 100 mM NaCl, HPTS (1 mM) at pH 7.2 and extravesicular solution contains 20 mM HEPES buffers, 100 mM NaX (where X⁻ = Cl⁻, NO₃⁻, F⁻, I⁻, Br⁻, SCN⁻, SO₄²⁻) at pH = 7.2.

5.2.4. Quantitative measurement of transport activity from chloride ISE assay — To find out the EC₅₀ value of all the compounds, the chloride-ISE-based Cl⁻/NO₃⁻ exchange assay was performed at varying concentrations. From these experiments, the chloride efflux (%) at 500s was plotted as a function of the carrier concentration (μM). The data points were fitted to the modified Hill equation using the Origin program 6.0.

$$Y = Start + (End - Start) \times \frac{X^n}{(K^n + X^n)} \dots\dots\dots (Eq.S2)$$

In this equation,

a = START = control value (DMSO),

b = END = 100,

Y is the chloride efflux efficiency at 500 s (%)

X is the carrier concentration (μM).

Where n is the Hill coefficient, EC₅₀ values at 500 s can be obtained directly from this modified Hill plot.

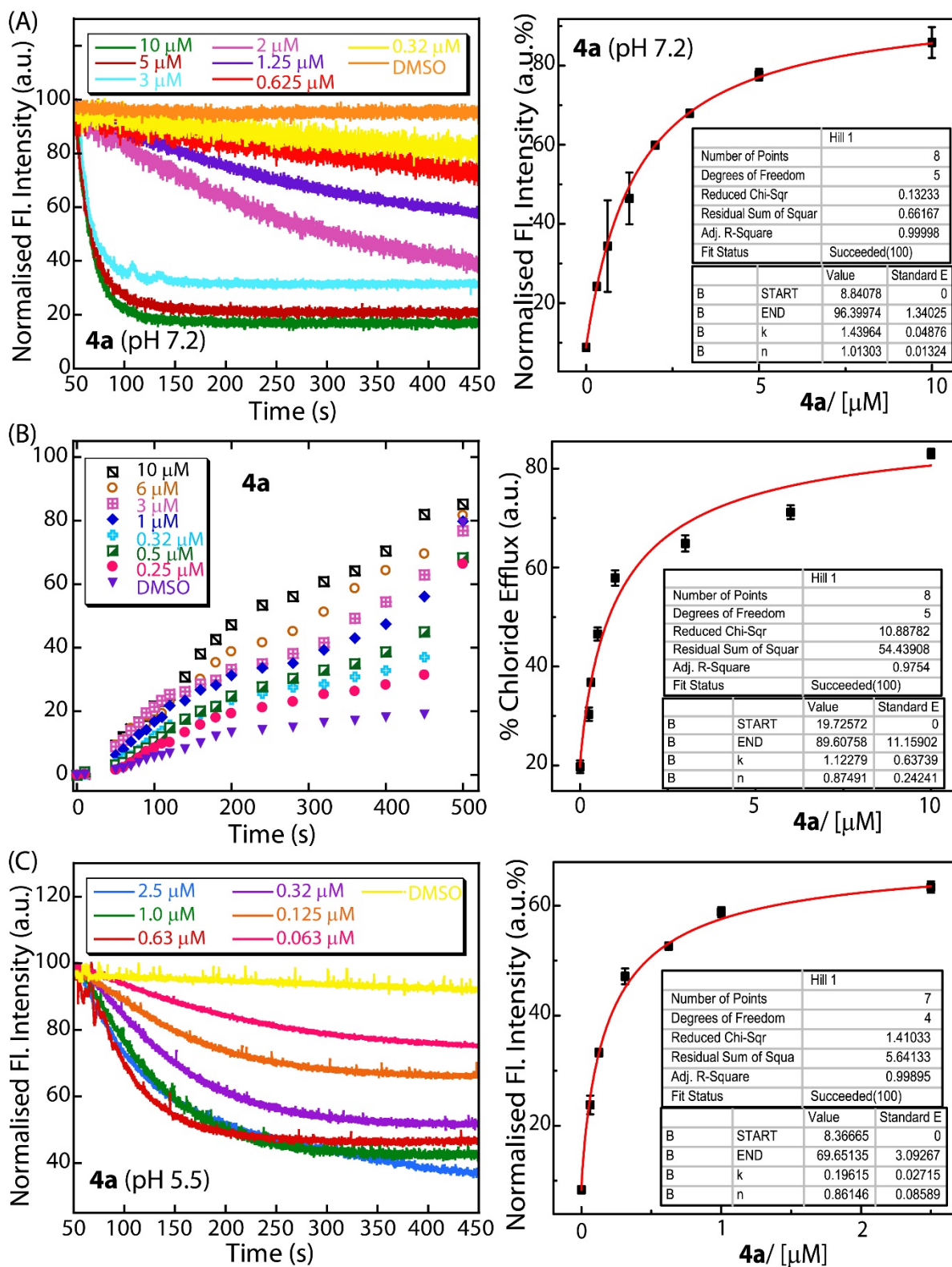


Fig. S7. Lucigenin-based concentration-dependent Cl^- transport properties of **4a** at pH 7.2 (A). Concentration-dependent ISE-based Cl^- efflux studies of **4a** at pH 7.2 (B). Lucigenin-based concentration-dependent Cl^- transport properties of **4a** at pH 5.5 (C).

6. Anion binding studies:**6.1. Anion binding analysis by ¹H-NMR titration:**

The ¹H NMR titration was performed for **4a** in DMSO-*d*₆. The stock solutions of the compound (10 mM) and TBACl (1.5 M) were prepared in DMSO-*d*₆. The tetrabutylammonium ammonium chloride salt was used as the source of chloride ions. The ¹H NMR titrations of the compound in DMSO-*d*₆ were performed by the subsequent addition of salt (0-15 equiv.). The changes in chemical shift ($\Delta\delta$) values of the N-H protons of the compounds were analyzed. MestReNova software was used to stack all the titration spectra. The BindFit v0.5 software fitted the changes in a chemical shift against the concentration of anions. The association constant (K_a) values were calculated using the BindFit v0.5 software (1:1 binding model).

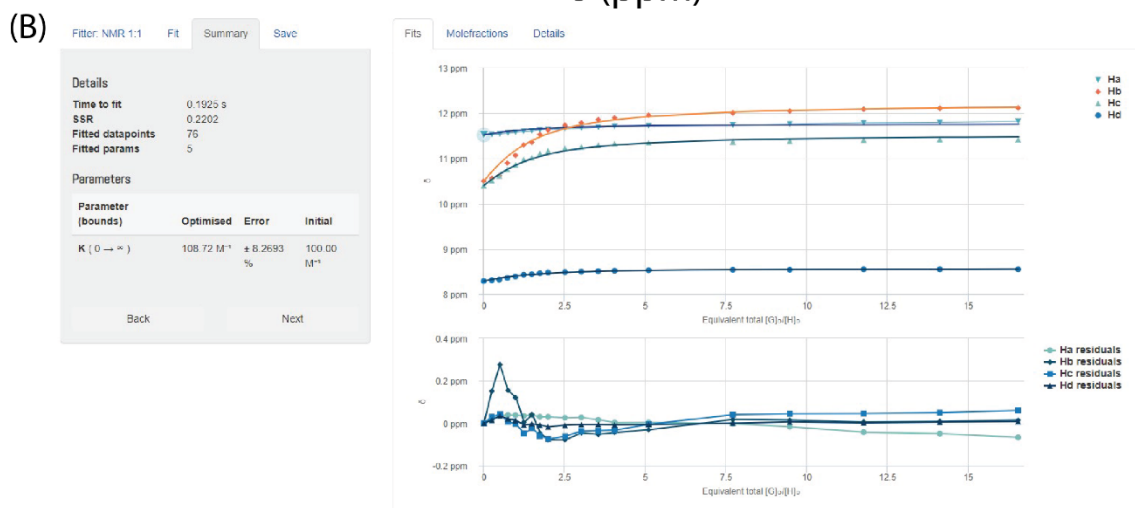
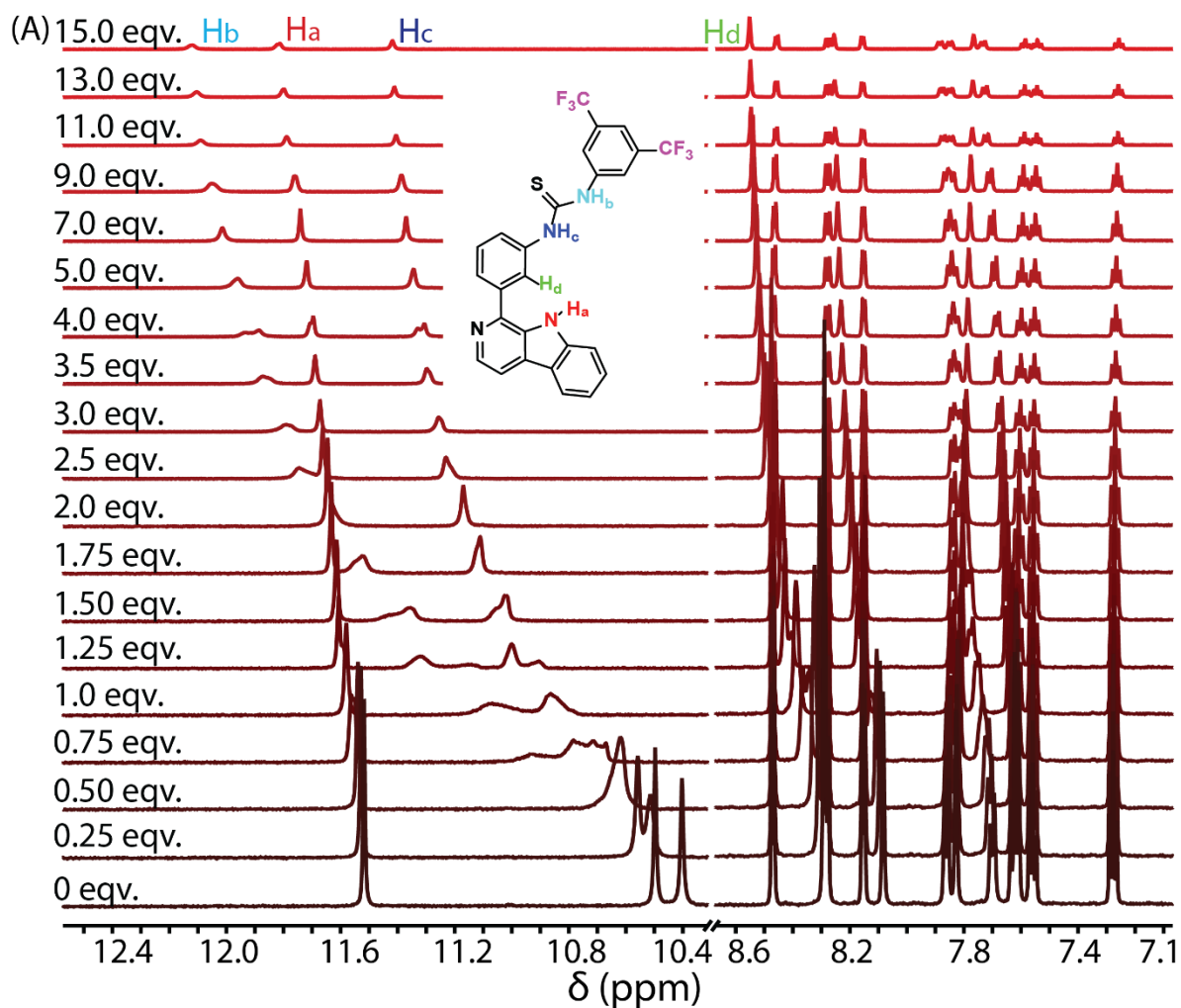


Fig. S8. ¹H NMR (600 MHz, rt) titration spectra for compound **4a** (10 mM) with TBACl in DMSO-*d*₆ solvent. The amounts of added TBACl are shown on the spectra (A). The plot of the concentration of TBACl versus the chemical shift of the ¹H signal was fitted using the 1:1 binding model of the Bindfit v0.5 program (B).

6.2. Chloride binding studies: Compound **4a** (1 mM) and TBACl (1 mM) were mixed in the ratio of **4a**:TBACl (1:1) in methanol. Then ESI-MS spectrum of the sample was taken. The data confirms the formation of **4a**.Cl⁻ (1:1) complex.

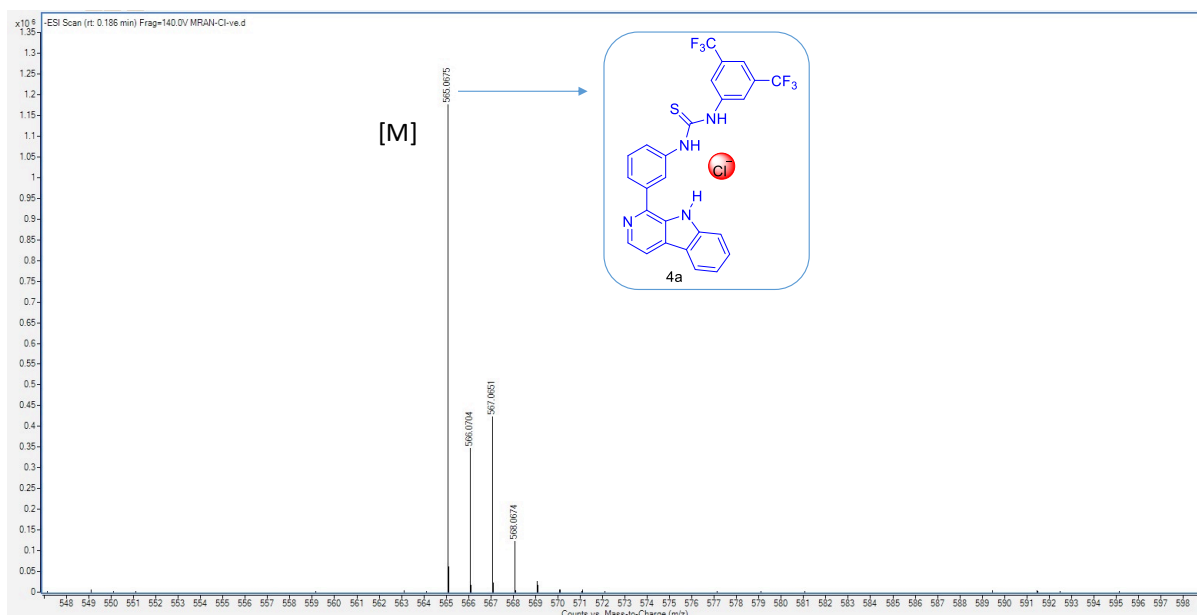


Fig. S9. ESI-MS spectrum of **4a**.Cl⁻ complex.

7. Mechanism of ion transport:

7.1. Transport activity in the presence of FCCP — The vesicles were prepared following the procedure discussed in the earlier section.¹⁰ The ion transport activity was measured in the absence and presence of FCCP (H⁺ selective transporter). First, 2920 μL of 20 mM HEPES buffer, pH 7.2, containing 100 mM NaCl and 50 μL of the EYPC/CHOL-LUV Δ lucigenin was taken in a 3 mL fluorescence cuvette, and the cuvette was placed in the fluorescence spectrophotometer at room temperature under mild stirring condition. After that, the compound (8 μL of the stock solution in DMSO) and 2 μL of FCCP solution in DMSO (1 μM) were added to the solution. The cuvette was then kept inside the fluorescence instrument under stirring conditions for 3 minutes to allow maximum incorporation of the compounds into the lipid bilayers. After that, the lucigenin fluorescence intensity was monitored (t = 0 sec) at 506 nm (λ_{ex} = 455 nm). After 450 sec, the kinetic experiment was terminated by adding 20 μL of 20% Triton-X100 solution (to rupture the vesicular arrangements) into the cuvette, and the fluorescent measurements were continued for another 50 sec (t = 500 sec). The control experiment was performed in the absence of FCCP.

7.2. Preferential ion transport activity in the presence of valinomycin (valinomycin assay)

— For the valinomycin assay, the EYPC/CHOLLUV \supset lucigenin was prepared by following a similar procedure as mentioned in the earlier section.¹¹ The extracellular buffer was replaced with 100 mM KCl with 100 mM NaNO₃. Here, at 50 s, performed as a solution, the respective compound (from DMSO stock) and /or 2 μ L valinomycin (12.0 pM) of 10 μ L was added to initiate the anion transport kinetics. The fluorescence emission intensity of the lucigenin dye was normalized at t = 50 and t = 500 s and transferred to 0 and 100 units, respectively.

7.3. Evidence for the carrier mechanism — Lucigenin assay using 1,2-dipalmitoylphosphatidylcholine (DPPC) was employed to determine the transport mechanism of the compounds.¹⁰ DPPC-LUV \supset lucigenin were prepared in 20 mM HEPES buffer pH 7.2, containing 100 mM NaNO₃. For the preparation of DPPC-LUV \supset lucigenin, the first 50 μ L of DPPC (100 mg/mL stock in de-acidified CHCl₃) was taken in a clean and dry glass vial, and the organic solvent was removed under reduced pressure (for 5-6 h) at room temperature. The dry, thin film was then hydrated with 600 μ L of 20 mM HEPES buffer, pH 7.2, containing 1 mM lucigenin and 100 mM NaNO₃. The solution was then sonicated for 30 min at 50 °C and was vortexed occasionally for 15-20 minutes. After that, the solution was subjected to a freeze-thaw cycle 12-13 times and again was sonicated 10 times (40-sec sonication followed by 20-sec incubations in ice water). The LUVs were prepared by extrusion using Avanti Mini-Extruder (Avanti Polar Lipids, Alabaster, AL) through 200 nm pore-size polycarbonate membranes according to the manufacturer's protocol. The unencapsulated dye was removed using a gel filtration (Sephadex G50) column with 20 mM HEPES buffer, pH 7.2, containing 100 mM NaNO₃. The final volume of the collected vesicle solution was adjusted to 500 μ L with 20 mM HEPES buffer pH 7.2 containing 100 mM NaNO₃. The final lipid concentration was 13.62 mM (assuming 100 % lipid regeneration). For the transport activity assay, the first 2920 μ L of 20 mM HEPES buffer, pH 7.2, containing 100 mM NaNO₃, 50 μ L of the DPPC-LUV \supset lucigenin (concentration of the stock solution was 13.62 mM), and 20 μ L of 5 M NaCl was taken in a 3 mL fluorescence cuvette, and the cuvette was placed in the fluorescence spectrophotometer under slow stirring conditions. After that, compounds (10 μ L from a 5 μ M stock solution in DMSO) were added to the solution to achieve a concentration ratio of 1: 25,000 for compound and lipids. The lucigenin fluorescence-based kinetic measurements were performed as mentioned above.

7.4. Transport Activity across DPPC-LUV \supset lucigenin (DPPC Assay) — DPPC assay was performed using a Fluoromax-4 spectrofluorometer (Horiba Scientific, Singapore) connected with a refrigerated system for temperature control (where the temperature was regulated using a temperature controller). In this assay, 2920 μL of 20 mM HEPES buffer, pH 7.2 containing 100 mM NaNO_3 , and 50 μL of the DPPC-LUV \supset lucigenin were taken in a 3 mL fluorescence cuvette. 10 μL of DMSO stock solution of compound **4a** was added to the cuvette (to make the anionophore and lipid ratio of 1: 25,000). The kinetic experiment was started (at $t = 0$ s), and lucigenin fluorescence emission was monitored, as mentioned above. The cuvette was then kept under stirring conditions, and the chamber temperature was set to 25 $^\circ\text{C}$. After 50 sec, NaCl (20 μL , 5 M) was added to initiate the Cl^- influx kinetics. Finally, to terminate the kinetic experiment, the vesicles were lysed by adding 20% Triton X-100 (20 μL) in the cuvette at $t = 450$ sec, and fluorescent measurements were continued for another 50 sec (i.e., up to $t = 500$ sec).

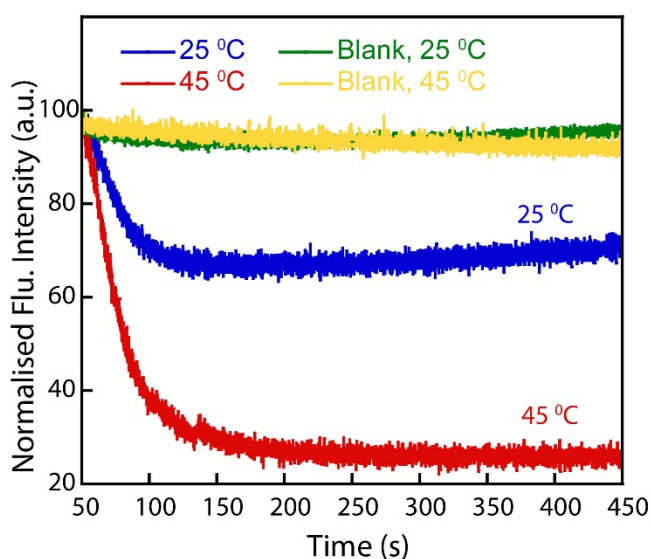


Fig. S10. Temperature-dependent lucigenin assay of compound **4a** across DPPC-LUV \supset lucigenin at 25 $^\circ\text{C}$ and 41 $^\circ\text{C}$.

7.5. U-tube experiment — The Classical U-tube experiment was performed according to the reported procedure to confirm the mechanistic pathway for the Cl^- transport by the compounds.¹² The lipid bilayer was mimicked using chloroform (12 mL) as the organic layer. The compound (2 mM) in chloroform was placed at the bottom of the U-tube with a mild stirring condition. The left arm of the tube was filled with 0.1 M aqueous HCl solution (10

mL), and the right one was filled with 0.1 M aqueous NaNO₃ solution (10 mL). The Cl⁻ concentration of the receiver end was monitored using a chloride-ISE. In the meantime, the pH of the receiver end was monitored using a pH meter. H⁺/Cl⁻ cotransport by the compound was observed by monitoring the right arm of the tube using both a pH meter and ISE.

7.6. Preparation of EYPC-LUV \Rightarrow carboxyfluorescein — A thin lipid film was prepared by evaporating a solution of 154 μ L EYPC (50 mg/mL stock in chloroform) and 39 μ L cholesterol (25 mg/mL stock in chloroform) in vacuo for 4 h.¹³ After that, lipid film was hydrated with 800 μ L buffer (10 mM HEPES, 10 mM NaCl, 50 mM carboxyfluorescein (CF), pH 7.2) for 1 h with occasional vortexing of 4–5 times and then subjected to freeze-thaw cycle (\geq 15 times). The vesicle solution was extruded through a polycarbonate membrane with 200 nm pores 19 times (has to be an odd number) to give vesicles with a mean diameter of \sim 200 nm. The extracellular dye was removed with size exclusion chromatography (Sephadex G-50) with 10 mM HEPES buffer (100 mM NaCl, pH 7.2.) Final concentration: \sim 25 mM EYPC-CHOL lipid; intravesicular solution: 10 mM HEPES, 10 mM NaCl, 50 mM CF, pH 7.2; extravesicular solution: 10 mM HEPES, 100 mM NaCl, pH 7.2.

7.7. Carboxyfluorescein leakage assay — In a clean and dry fluorescence cuvette, 50 μ L of the above lipid solution and 2940 μ L of 10 mM HEPES buffer 100 mM NaCl, pH 7.2 was taken and kept in slowly stirring condition by a magnetic stirrer equipped with the fluorescence instrument (at $t = 0$ s). The CF fluorescence emission intensity time course, F_t , was observed at $\lambda_{em} = 517$ nm ($\lambda_{ex} = 492$ nm). Compound **4a** was added at $t = 50$ s, and at $t = 450$ s, 20 μ L of 20% Triton X-100 was added to lyse those vesicles for 100% chloride influx. This study confirmed that the integrity of the bilayer membranes is intact in the presence of compound **4a**.

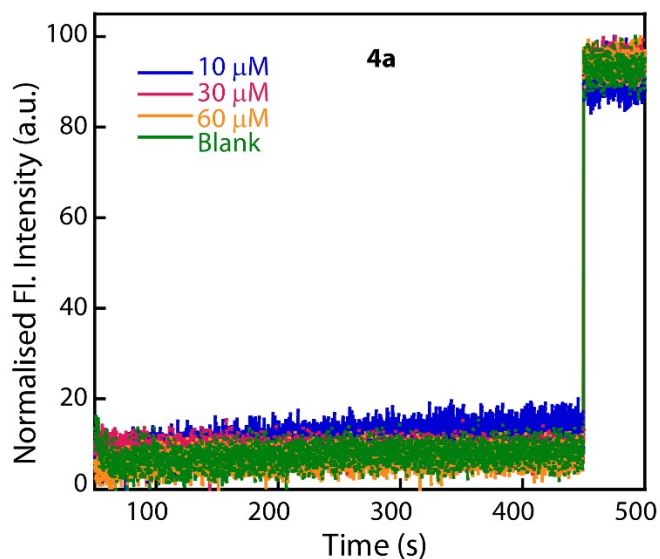


Fig. S11. Carboxy fluorescein leakage assay of compound **4a** across EYPC-LUV Δ carboxyfluorescein.

8. Theoretical studies:

8.1. Simulation setup — To determine the ion-bound structure of the molecule in acidic and neutral conditions, the molecule in both conditions was initially optimized independently along with one Cl⁻ ion using the B3LYP density functional theory (DFT)¹⁴ method in the Gaussian 09 program package. The force field parameters for both drugs were generated using the CHARMM General Force Field (CGenFF) with the ParamChem server.¹⁵⁻¹⁷ The optimized structure was placed on the top (20 Å away from the phosphate plane) of a 1,2-dipalmitoyl-sn-phosphocholine (DPPC) bilayer. The system was then solvated with TIP3P water¹⁸ and neutralized. Each step of the system-building process was carried out using the Membrane Builder module of CHARMM-GUI.¹⁹ The final system contained ~40,000 atoms with dimensions of 60×60×110 Å³, for both conditions. The prepared systems were minimized using the steepest descent algorithm for 5,000 steps, followed by molecular dynamics (MD) equilibration of 2 ns. Then for both conditions, 5 replicates of steered MD simulations were performed to pull the molecule through the membrane with a force constant of 10 kcal/mol/Å². During simulations, hydrogen bonds, captured during DFT optimization between the Cl⁻ and three protons of the molecule, were constrained. These bond constraints were needed since classical forcefield parameters are not well optimized to keep the ions bound to the molecule during MD simulation.

8.2. MD simulation protocol — MD simulations in this study were performed using NAMD 2.14^{20, 21} utilizing CHARMM36²² and CGenFF¹⁵⁻¹⁷ force field parameters for lipids and the molecule, respectively. Bonded and short-range nonbonded interactions were calculated every 2 fs and periodic boundary conditions were employed in all three dimensions. The particle mesh Ewald (PME) method²³ was used to calculate long-range electrostatic interactions every 4 fs with a grid density of 1 \AA^{-3} . A force-based smoothing function was employed for pairwise nonbonded interactions at a distance of 10 \AA with a cutoff of 12 \AA . Pairs of atoms whose interactions were evaluated were searched and updated every 20 fs. A cutoff (13.5 \AA) slightly longer than the nonbonded cutoff was applied to search for the interacting atom pairs. Constant pressure was maintained at a target of 1 atm using the Nosé-Hoover Langevin piston method.^{24, 25} Langevin dynamics maintained a constant temperature of 310 K with a damping coefficient, γ of 0.5 ps^{-1} applied to all atoms. Simulation trajectories were collected every 10 ps.

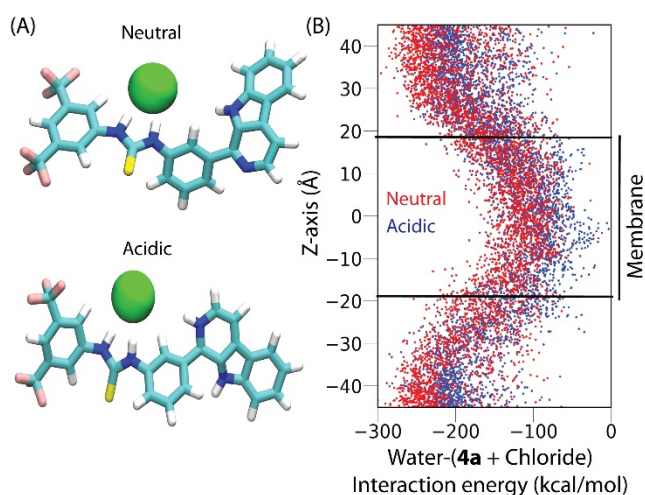


Fig. S12. The Cl⁻-bound structure of **4a** in neutral and acidic conditions is derived using DFT-based QM geometry optimization. Hydrogen bonds were highlighted with dotted lines (A). Water-ligand interaction energy along the permeation event of **4a** both in acidic and neutral conditions (B). Data points are collected for all the replicates of the steered MD simulation.

9. Fluorescence-based regeneration assay with photo-irradiation:

9.1. UV spectra for compounds 4a and 5 — The UV spectra for compounds **4a** and **5** were measured using spectrophotometer. Both the compounds were measured in water with $20 \mu\text{M}$ concentration.

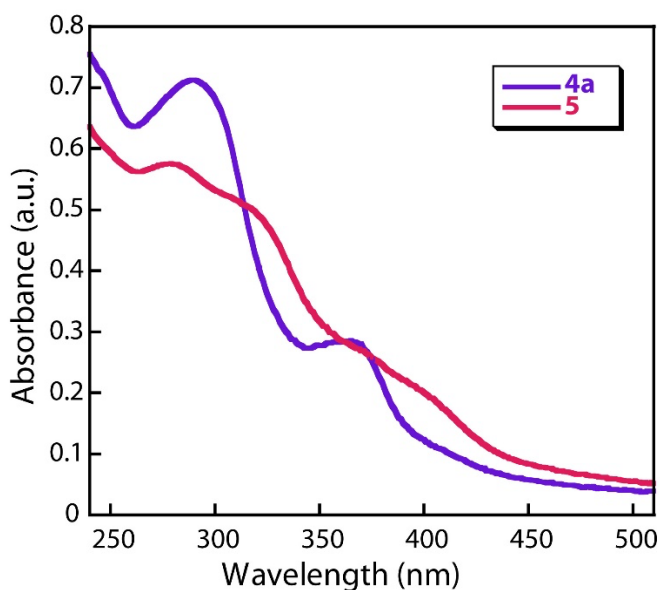


Fig. S13. UV-Vis spectra of compounds **4a** and **5**.

9.2. HPLC-based anionophore regeneration from pro-anionophore using photo-irradiation

— In order to confirm the regeneration of active ionophore **4a** from proanionophore **5**, HPLC analysis was performed. Proionophore (10 μM) was irradiated in the PBS buffer system with 365 nm at various time intervals (0 min, 5 min, 12 min, 20 min, 30 min, 45 min). A time-dependent study confirms the successful release of **4a** and *4-formyl-3-nitrosobenzoic acid* (**6**) from proionophore **5**, which was confirmed by measuring HRMS. To check the stability of the proionophore, we have recorded spectra of compound **5** over the time interval of 45 min. (Experiments were performed under dark) Column used: Ascentis® express C18, 2.7 μm HPLC column, flow rate: 1.0 mL/min, mobile phase used: Optimized gradient of PBS buffer/methanol. The gradient used: 0-5 min- 20% buffer:80% CH_3OH , 5-8 min- 0% buffer:100% CH_3OH , 8-12 min- 5% buffer:95% CH_3OH , 12-15 min- 20% buffer:80% CH_3OH .

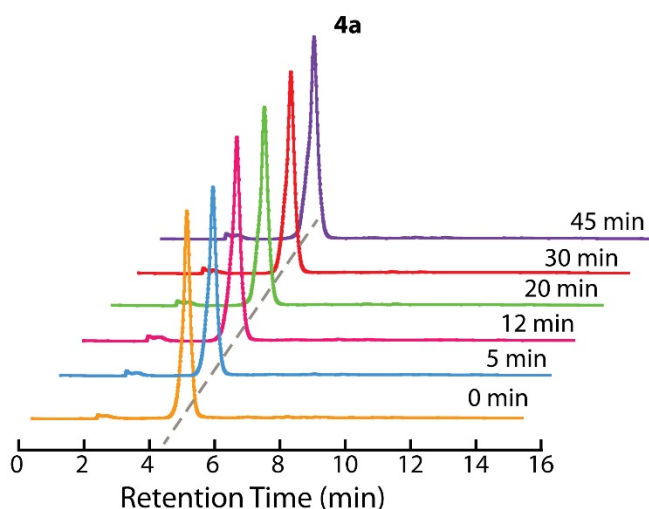


Fig. S14. HPLC traces of **4a** after light irradiation at different time intervals.

9.3. Ion transport studies of the regenerated compound — Irradiation of **5** in an ex-situ manner using 365 nm light was conducted with 10 μM compound **5** in DMSO stock. The protocol of the study performed was according to the earlier section 4.1.2. In the whole transport process, the concentration of compound **5** was kept constant, and the irradiation time was varied.²⁶ The experiment added LUVs containing lucigenin (intravesicular: 20 mM HEPES and 100 mM NaNO_3) to the buffer (extravesicular: 20 mM HEPES and 100 mM NaCl) and stirred. An irradiated sample of compound **5** under 365 nm light was added in 50 s, and spectra were recorded for the next 400 s. At $t = 450\text{s}$, 20 μL of 20% Triton X-100 was added to lyse the vesicle for 100% quenching of the dye. (The irradiation time was 5, 10, 18, and 30 minutes).

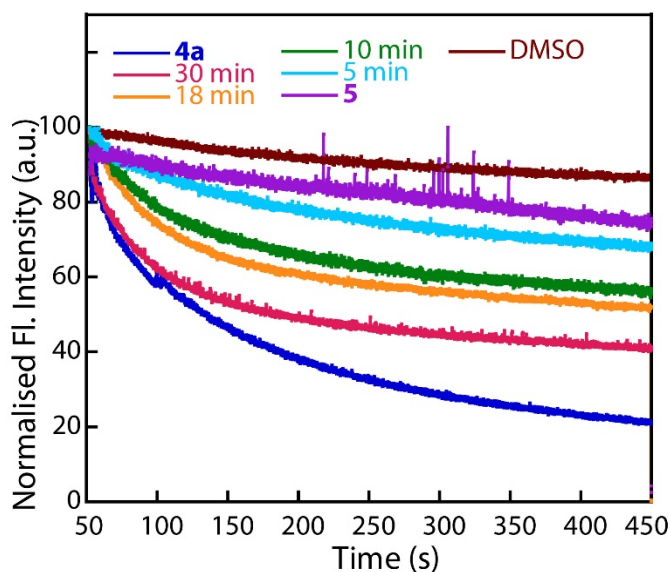


Fig. S15. Cl^- transport properties of proanionophore **5** before and after light treatments (at different intervals). Light treatment of proanionophore **5** confirms the regeneration of active anionophore **4a**.

9.4. Insitu-light treated chloride efflux study of compound **5** across EYPC/CHOL-LUV

— To measure the extent of efflux of Cl^- with in-situ light irradiation on compound **5**, the EYPC/CHOL-LUVs (50 μL) and 5 mM phosphate buffer, pH 7.2, containing 100 mM NaNO_3 (3940 μL) were taken in a clean and dry glass vial and kept under mild stirring condition. The chloride electrode was immersed into the solution under mild stirring conditions. To initiate the Cl^- transport kinetics at $t = 50$ s, 10 μL of compound **5** (from DMSO stock solution) was added into the stirring solution, and the readings were noted from the ion meter. Then, after 80 s, 365 nm light was irradiated on the sample and readings were measured for 15 minutes. After 15 minutes, the vesicles were lysed using 50 μL of 20% Triton X-100 solution. The total Cl^- efflux reading was taken at the 18th minute (allowing complete disruption of the LUVs). Thus, we have measured the release of anionophore from proanionophore **5** at different concentrations of 20 μM , 15 μM , 10 μM and 7.5 μM . The initial reading was considered 0% Cl^- efflux, and the final reading at 18 min was considered 100% Cl^- efflux.

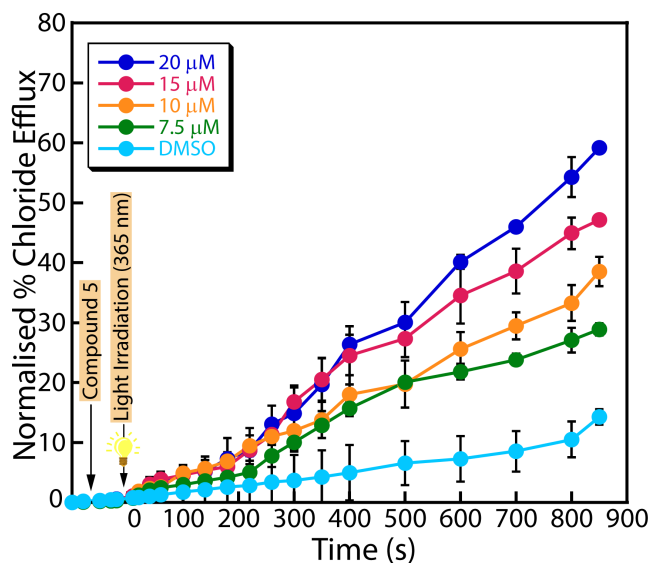


Fig. S16: Concentration-dependent in-situ light irradiation on **5** and generation of **4a** in ISE-based Cl^- efflux studies.

10. Cellular activity studies:

10.1. MTT Assay — MCF-7, MDA-MB-231 and MCF-10A cells were seeded on 96 well plates (10^4 cells) and incubated at 37°C and 5% CO_2 incubator for 24 h. Cells were then treated with complete media containing different concentrations (0, 0.1, 1, 10, 25, 50, 75, 100 μM) of compounds in triplicate and incubated for 48 h. After 48 h, 20 μl of MTT solution (5mg/ml in 1X PBS) was added to each well and incubated for 4 h in an incubator. After that, MTT-containing media were removed, and 100 μL of MTT solvent containing 100 % isopropanol, 4 mM HCl, and 0.1 % triton X-100 were added to each well. Plates were then incubated for 15 minutes at room temperature in the dark with slight shaking. Finally, the absorbance was measured in a microplate reader (Multiskan™ GO) at 570 nm wavelength. Human breast epithelial cell line MCF10A was a kind gift from Prof. Michael R. Green (University of Massachusetts Medical School, USA). Human breast cancer cell lines MCF7 and MDA-MB-231 were obtained from National Centre for Cell Science (NCCS), India cell repository.

10.2. HBSS Assay — HBSS assay was performed in the presence or absence of Cl^- in HBSS (Hank's Balanced Salt Solution) buffer. MCF-7 cells were seeded on 96 well plates and incubated for 24 h in a 37°C , 5 % CO_2 incubator. Media were replaced by HBSS buffer (with or without Cl^-) containing 10 % FBS and different concentrations of compound (0, 0.1, 1, 10, 25 μM) and incubated for 24 h. 20 μL of MTT solution (5mg/ml of 1X PBS) were added in each well and incubated for 4 h. MTT solution containing media was removed, and 100 μL of

a solution containing 100% isopropanol, 0.1% triton X100, 4mM HCl were added to each well for 15 mins at room temperature. The absorbance (OD) was taken at 570 nm in a microplate reader (Multiskan GO). All the experiments were performed in triplicate. HBSS buffer contains the following components:

HBSS with Cl⁻ composition: 136.9 mM NaCl, 5.5 mM KCl, 0.34 mM Na₂HPO₄, 0.44 mM KH₂PO₄, 0.81 mM MgSO₄, 1.25 mM CaCl₂, 5.5 mM D-glucose, 4.2 mM NaHCO₃ and 10 mM HEPES (pH 7.4).

HBSS without Cl⁻ composition: 136.9 mM Na-gluconate, 5.5 mM K-gluconate, 0.34 mM Na₂HPO₄, 0.44 mM KH₂PO₄, 0.81 mM MgSO₄, 1.25 mM Ca-gluconate, 5.5 mM D-glucose, 4.2 mM NaHCO₃ and 10 mM HEPES (pH 7.4).

10.3. SDS-PAGE and western blot studies — MCF7 (0.3×10^6) cells were seeded on 35 mm plates and allowed to grow for 24 h. The next day, cells were grown in the absence and presence of 10 μ M MR for 48 h. After 48 h of treatment, cells were collected, washed with ice-cold PBS and lysed with cell lysis buffer (50 mM Tris pH7.4, 250mM NaCl, 5 mM EDTA, 50 mM NaF, 0.5mM Na₃VO₄, 0.5% Triton X-100, and protease inhibitor cocktail) in ice for 30 min. Lysate was centrifuged at 20000xg for 30 mins. Protein-containing supernatants were collected, and protein concentration was measured using the Bradford method. The required amount of proteins was diluted in SDS sample buffer and boiled for 5 min. The samples were run on SDS PAGE and transferred onto the activated PVDF membrane. PVDF membrane was then blocked with either 5% non-fat milk or 5% BSA made in TBST buffer. After blocking, the membrane was washed with TBST buffer and incubated with primary antibody overnight at 4 °C with gentle rocking. The next day, the membrane was washed with TBST buffer and incubated with HRP-conjugated secondary antibodies for 2 h. Finally, the membrane was washed with TBST, and then blots were developed using chemiluminescence reagents from Pierce in GE AMERSHAM Image Quant 800.

10.4. Phototriggered cell death — Proionophore **5** was photoirradiated for 5, 15 and 30 mins using 365 nm UV light (4 watts). Irradiated and non-irradiated proionophore **5** was then treated to MCF7 cells seeded on 96 well plates for 48 h. 20 μ L of MTT solution (5 mg/mL of 1X PBS) were added in each well and incubated for 4 h. MTT solution containing media was removed, and 100 μ L of a solution containing 100 % isopropanol, 0.1 % triton X-100, 4 mM HCl were

added to each well for 15 mins at room temperature. The absorbance (OD) was taken at 570 nm in a microplate reader (Multiskan GO).

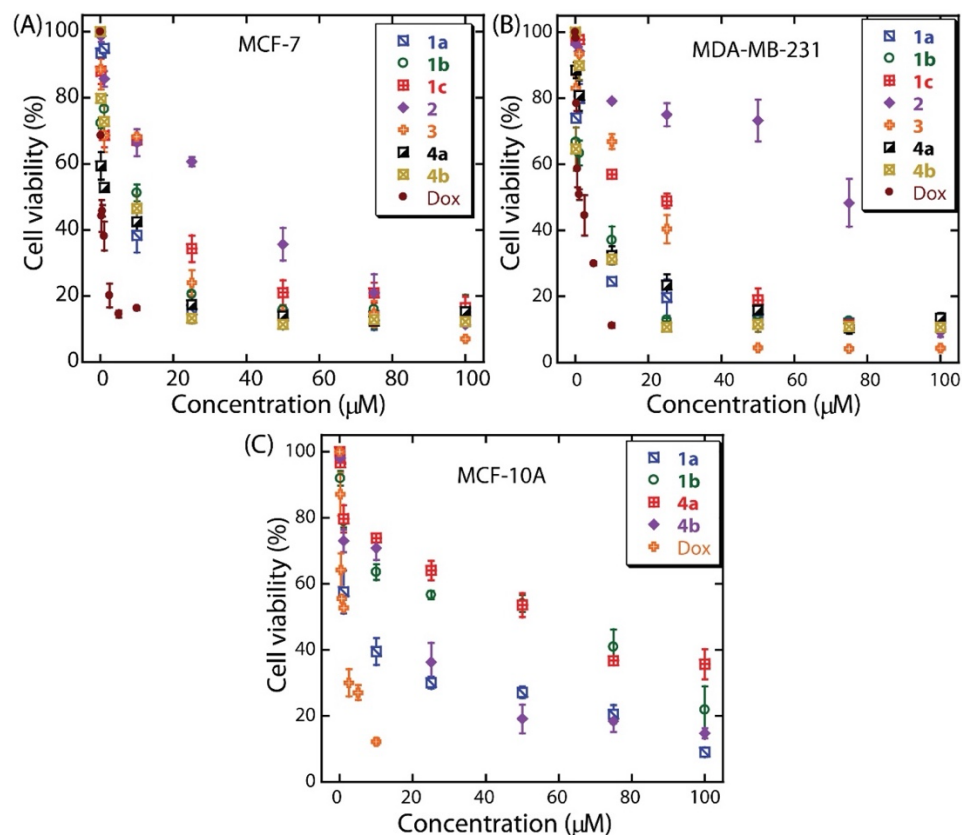


Fig. S17. Dose-dependent cell viability (48 h) of compound-treated MCF-7 (A), MDA-MB-231 (B) and MCF-10A (C) cell lines. All measurements were performed in triplicates.

Note: The β -carboline and tetrahydro- β -carboline-based compounds are known for DNA intercalation and topoisomerase inhibition, thus inducing cancer cell death. The tetrahydro β -carboline-based compounds also showed anticancer activity against a variety of cancer cell lines such as A59 (lung), PC-3 (prostate), HeLa (cervical) and MCF-7 (breast cancer). The derivatives of tetrahydro- β -carboline are also reported as inhibitors of enzymes like kinesin (Eg5) and topoisomerase, etc. The tetrahydro- β -carboline-based compounds also regulate cell cycle progression, inhibiting cancer cell proliferation.^{27, 28} Compounds **1a** and **1b** have structural similarities with tetrahydro- β -carboline, which has inherent anticancer activity, but due to lack of planarity, it does not have a suitable binding cavity for Cl^- . Hence, these compounds showed lower H^+/Cl^- transport activities, whereas they displayed higher cytotoxicity. The Cl^- dependent anticancer studies showed the relationship between Cl^- transport activities and anticancer activities. These results also suggest the Cl^- transport properties of the compounds are one of the probable pathways for its anticancer activities. It

might have another mechanism of anticancer activities, which require additional cellular and biochemical studies.

11. NMR spectra of synthesized compounds:

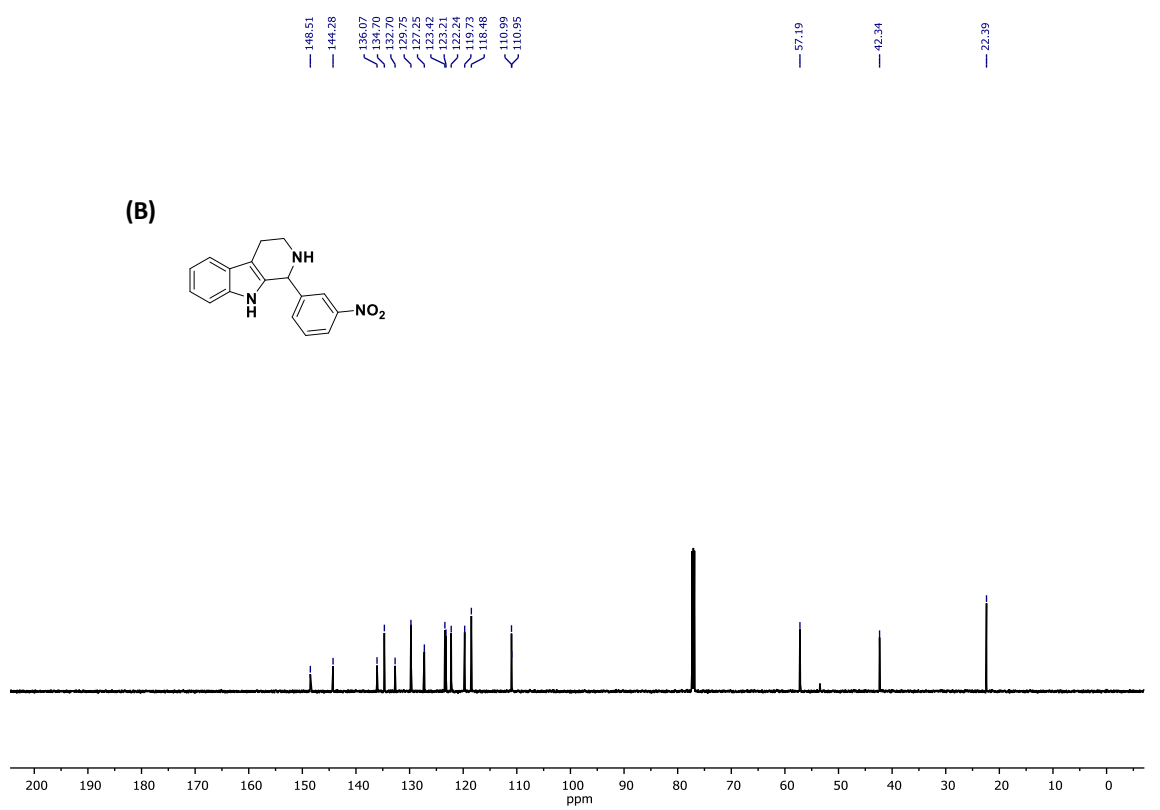
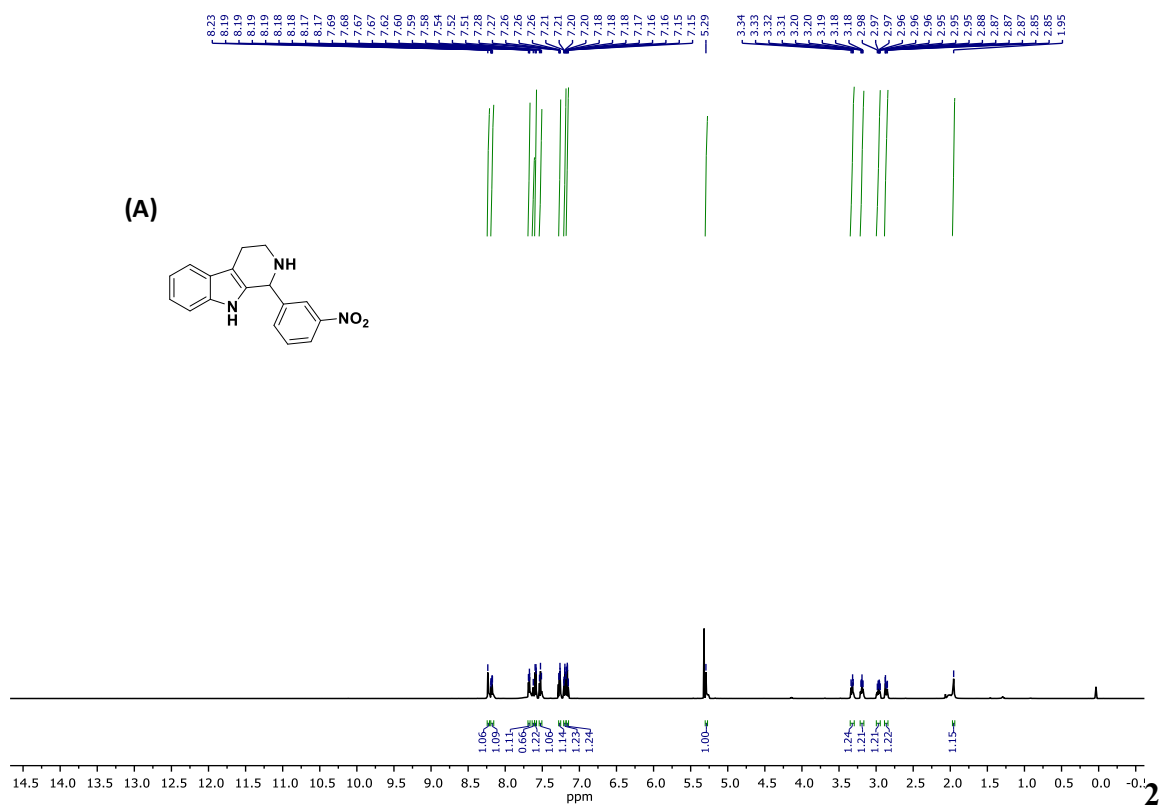


Fig. S18. ^1H NMR (A) and ^{13}C NMR (B) spectra of 1-(3-nitrophenyl)-2,3,4,9-tetrahydro-1*H*-pyrido[3,4-*b*]indole in the CDCl_3 solvent.

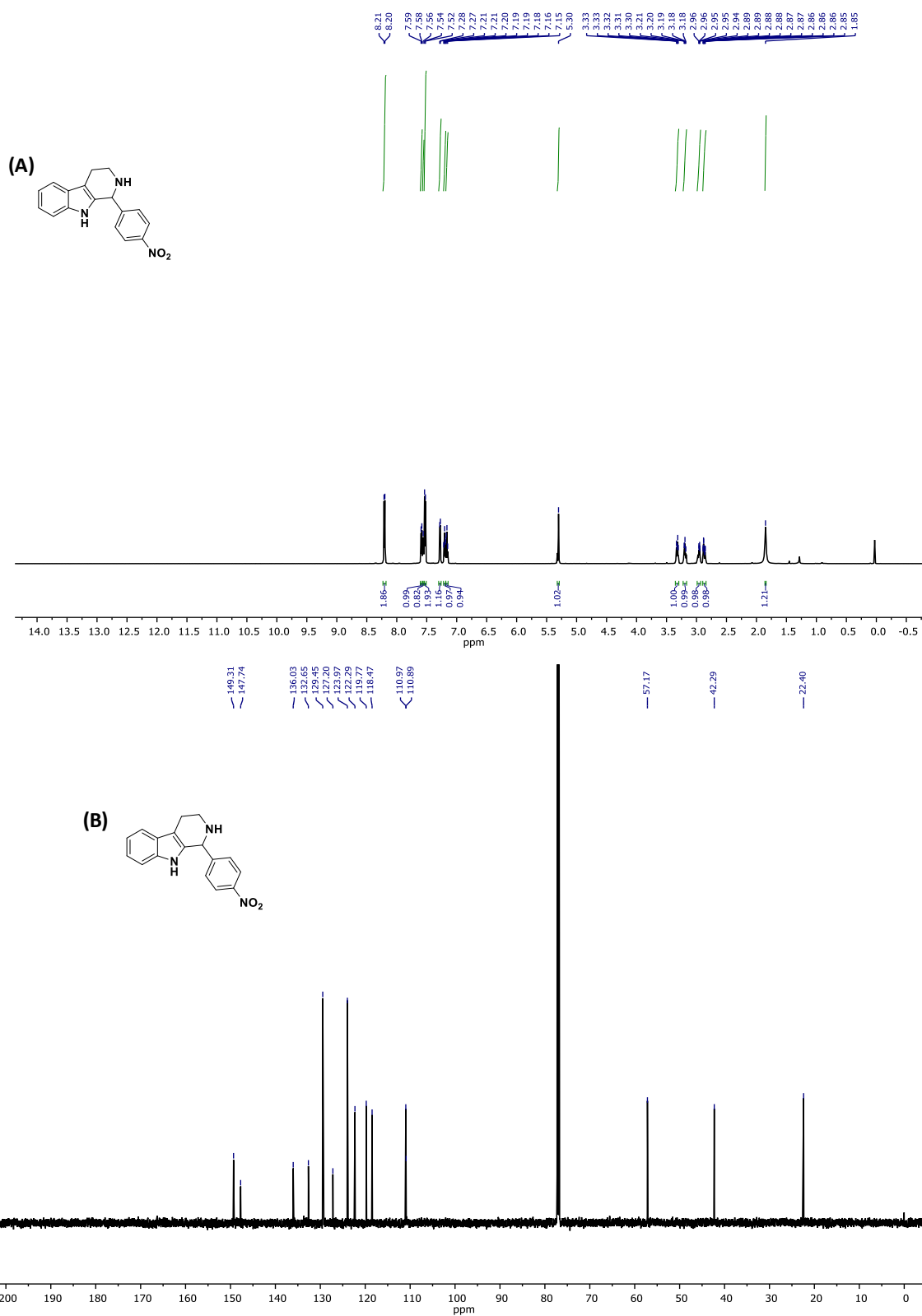


Fig. S19. ^1H NMR (A) and ^{13}C NMR (B) spectra of 1-(4-nitrophenyl)-2,3,4,9-tetrahydro-1*H*-pyrido[3,4-*b*]indole in the CDCl_3 solvent.

SUPPORTING INFORMATION

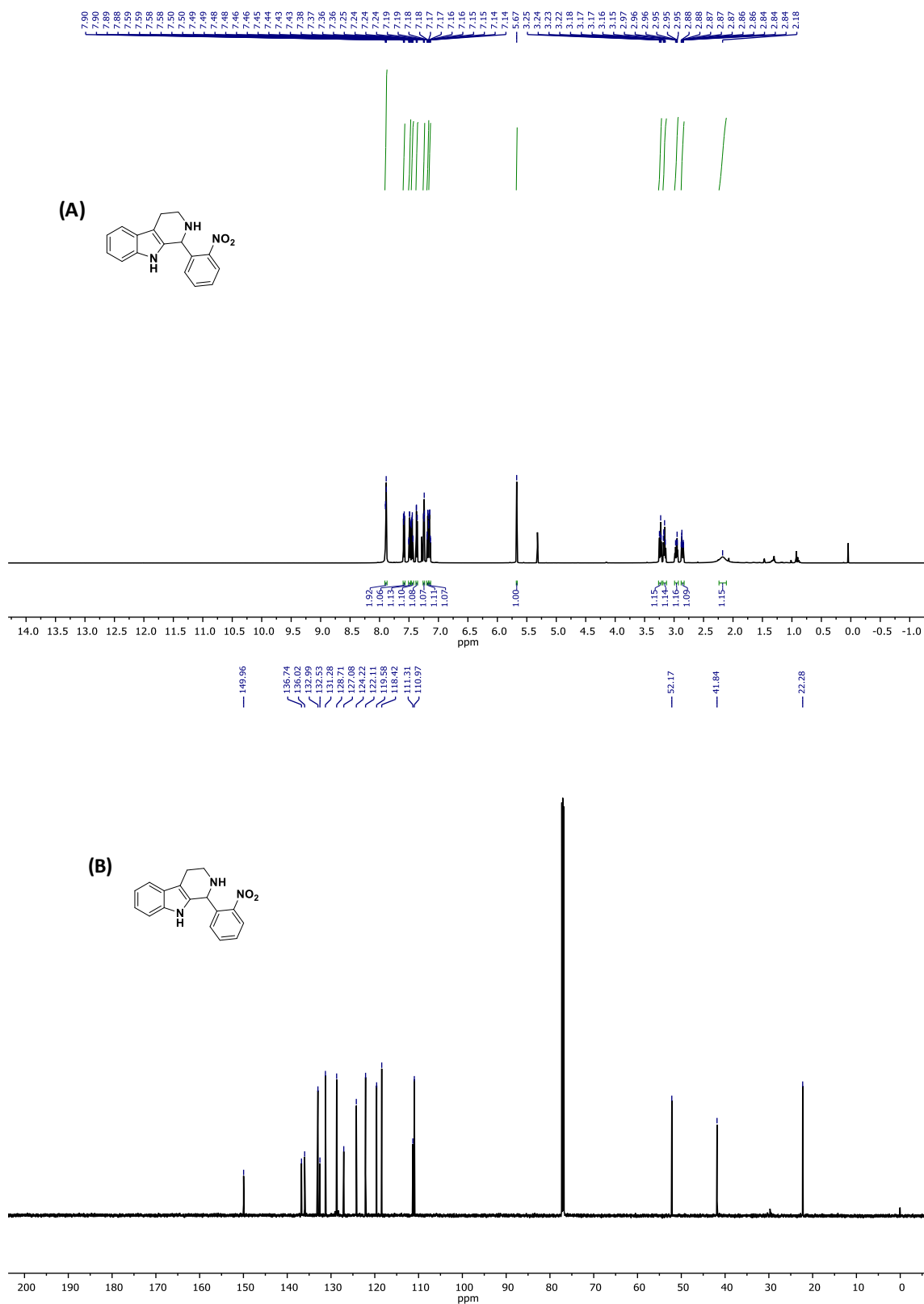


Fig. S20. ¹H NMR (A) and ¹³C NMR (B) spectra of 1-(2-nitrophenyl)-2,3,4,9-tetrahydro-1H-pyrido[3,4-b]indole in the CDCl₃ solvent.

SUPPORTING INFORMATION

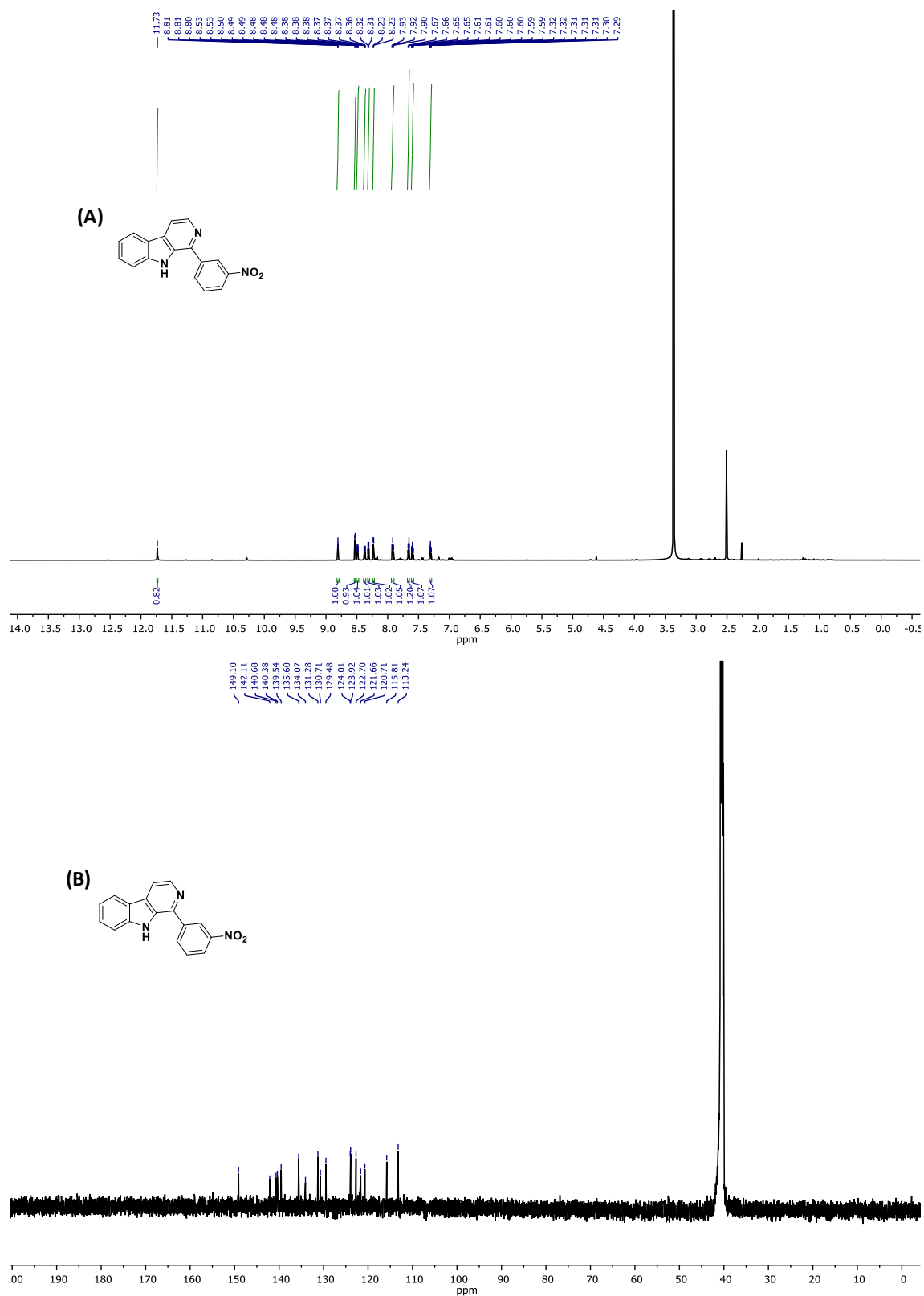


Fig. S21. ¹H NMR (A) and ¹³C NMR (B) spectra of 1-(3-nitrophenyl)-9H-pyrido[3,4-b]indole in the DMSO-*d*₆ solvent.

SUPPORTING INFORMATION

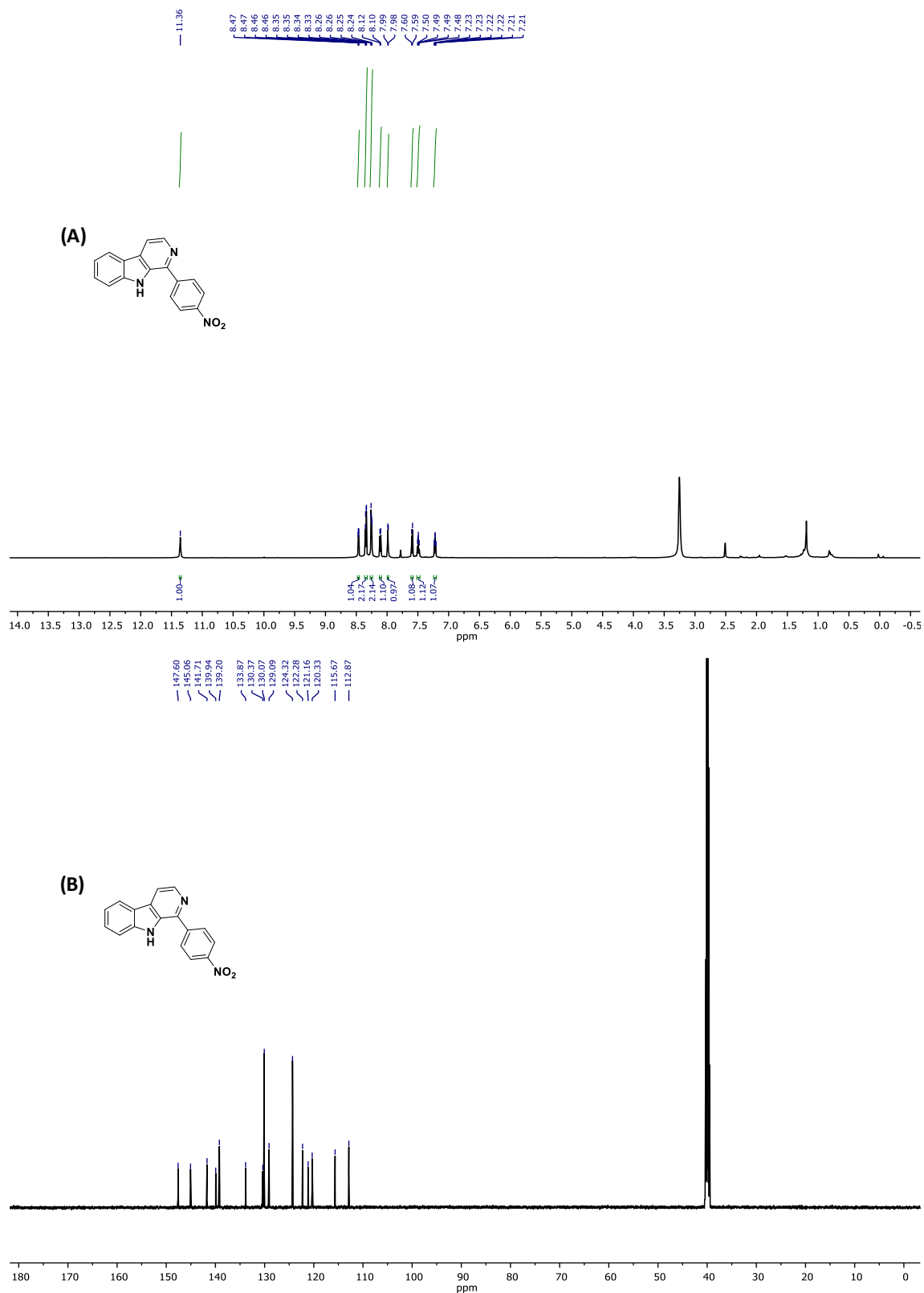


Fig. S22. ^1H NMR (A) and ^{13}C NMR (B) spectra of 1-(4-nitrophenyl)-9H-pyrido[3,4-b]indole in the $\text{DMSO-}d_6$ solvent.

SUPPORTING INFORMATION

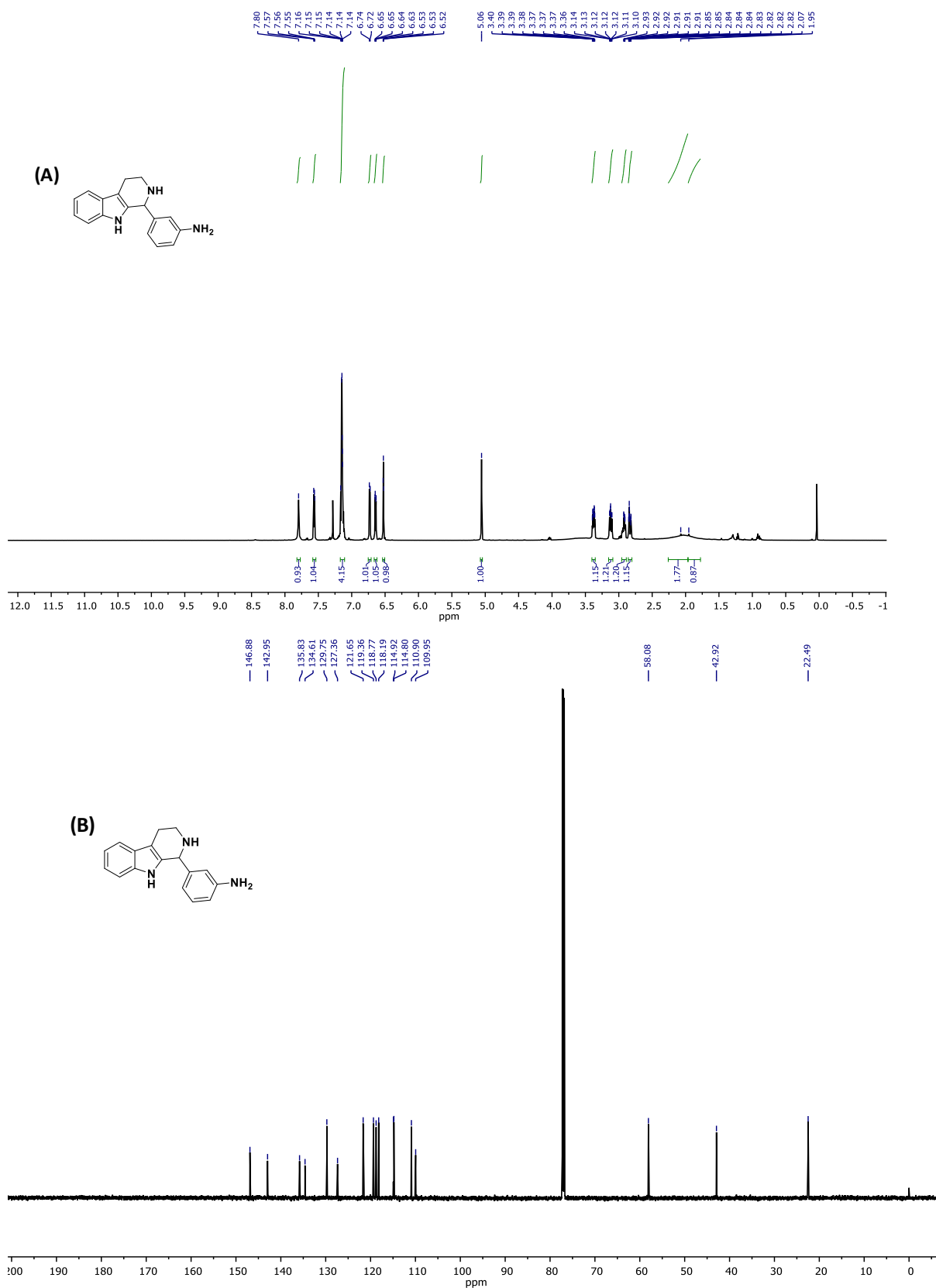


Fig. S24. ^1H NMR (A) and ^{13}C NMR (B) spectra of 3-(2,3,4,9-tetrahydro-1H-pyrido[3,4-b]indol-1-yl)aniline in the CDCl_3 solvent.

SUPPORTING INFORMATION

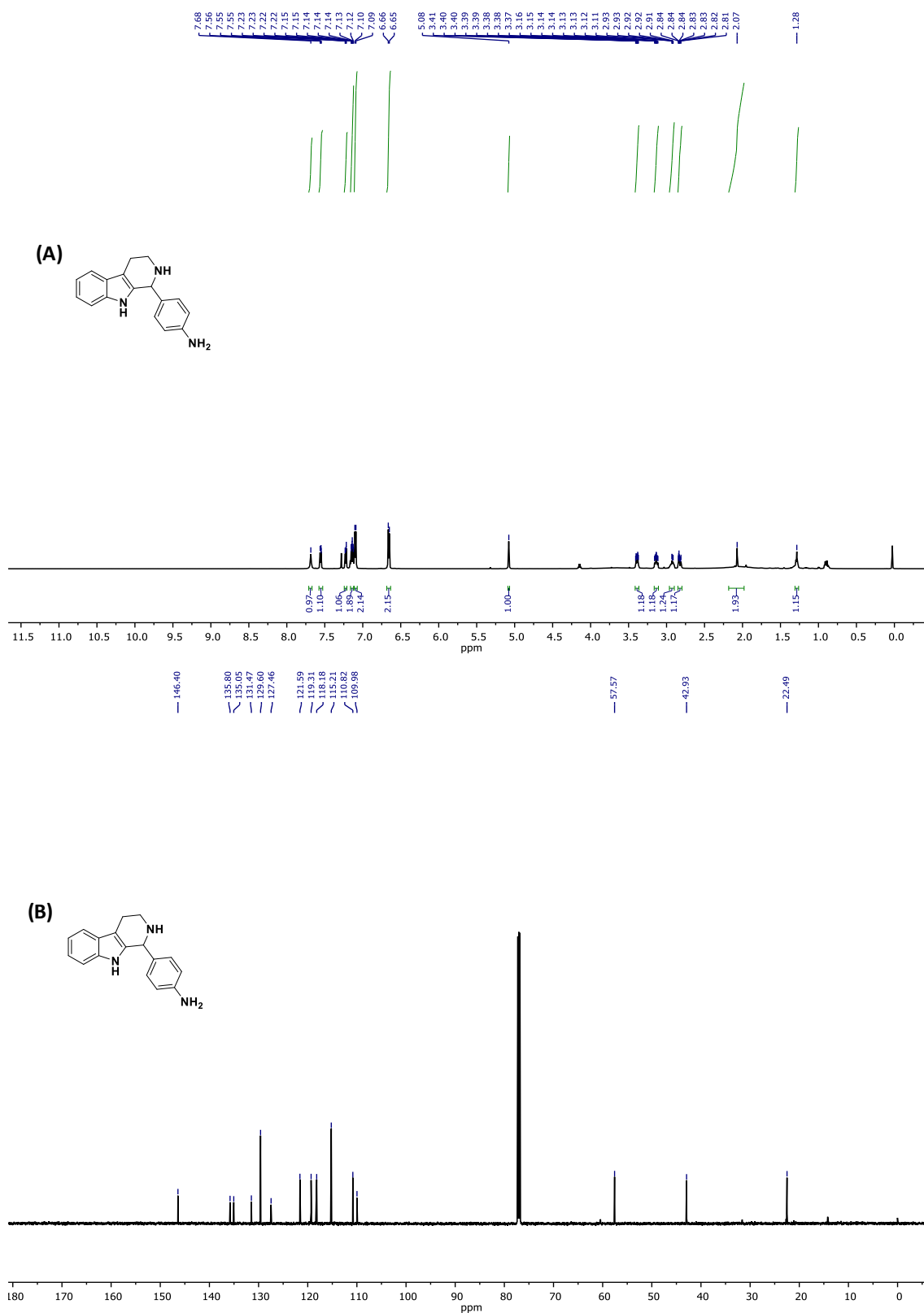


Fig. S25. ^1H NMR (A) and ^{13}C NMR (B) spectra of 4-(2,3,4,9-tetrahydro-1H-pyrido[3,4-b]indol-1-yl)aniline in the CDCl_3 solvent.

SUPPORTING INFORMATION

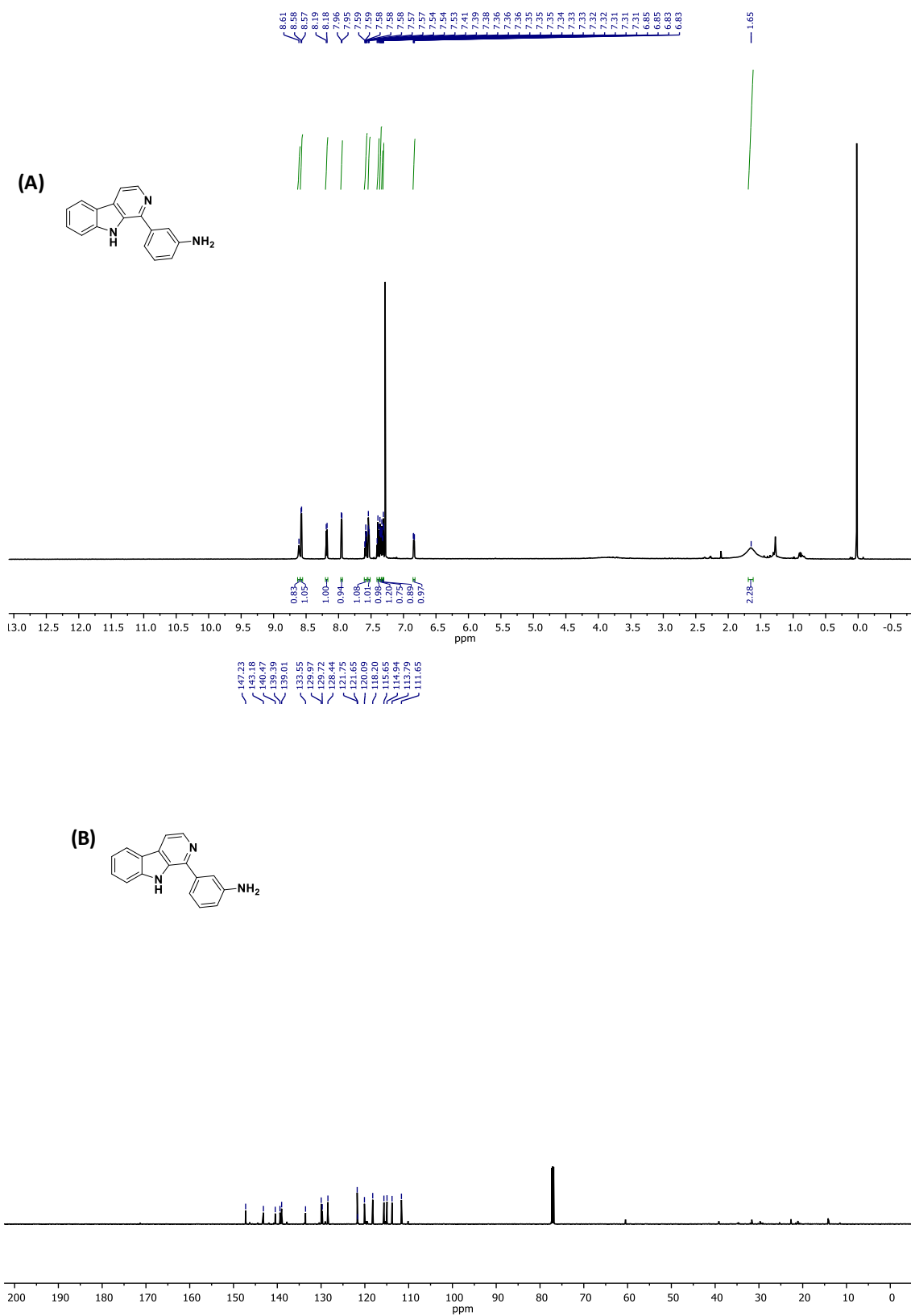


Fig. S26. ¹H NMR (A) and ¹³C NMR (B) spectra of 3-(9H-pyrido[3,4-b]indol-1-yl)aniline in the CDCl₃ solvent.

SUPPORTING INFORMATION

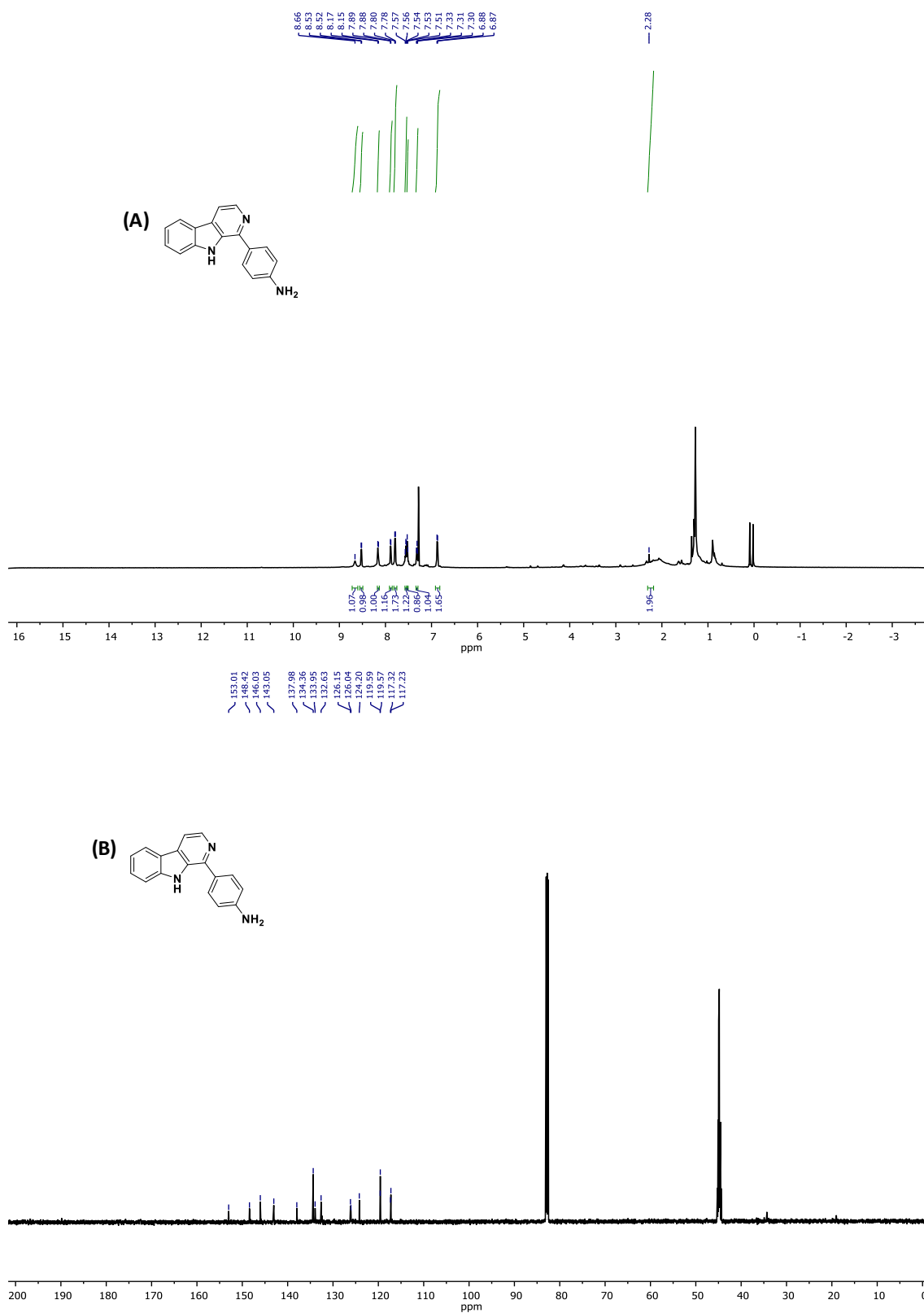


Fig. S27. ¹H NMR (A) and ¹³C NMR (B) spectra of 4-(9H-pyrido[3,4-b]indol-1-yl)aniline in the CDCl₃ + DMSO-*d*₆ solvent mixture.

SUPPORTING INFORMATION

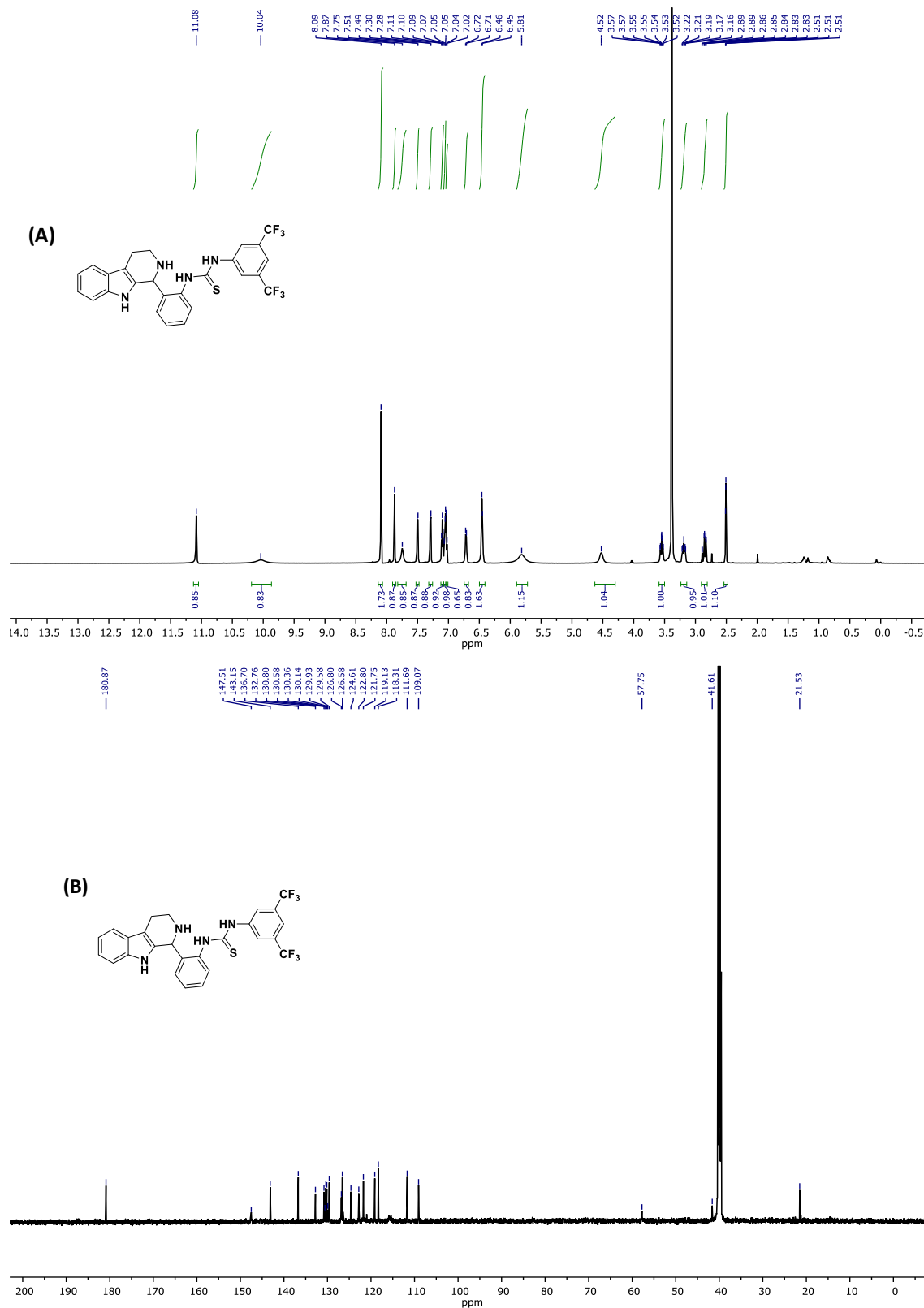


Fig. S28. ¹H NMR (A) and ¹³C NMR (B) spectra of 1-(3,5-bis(trifluoromethyl)phenyl)-3-(2-(2,3,4,9-tetrahydro-1H-pyrido[3,4-b]indol-1-yl)phenyl)thiourea (**1a**) in the DMSO-*d*₆ solvent.

SUPPORTING INFORMATION

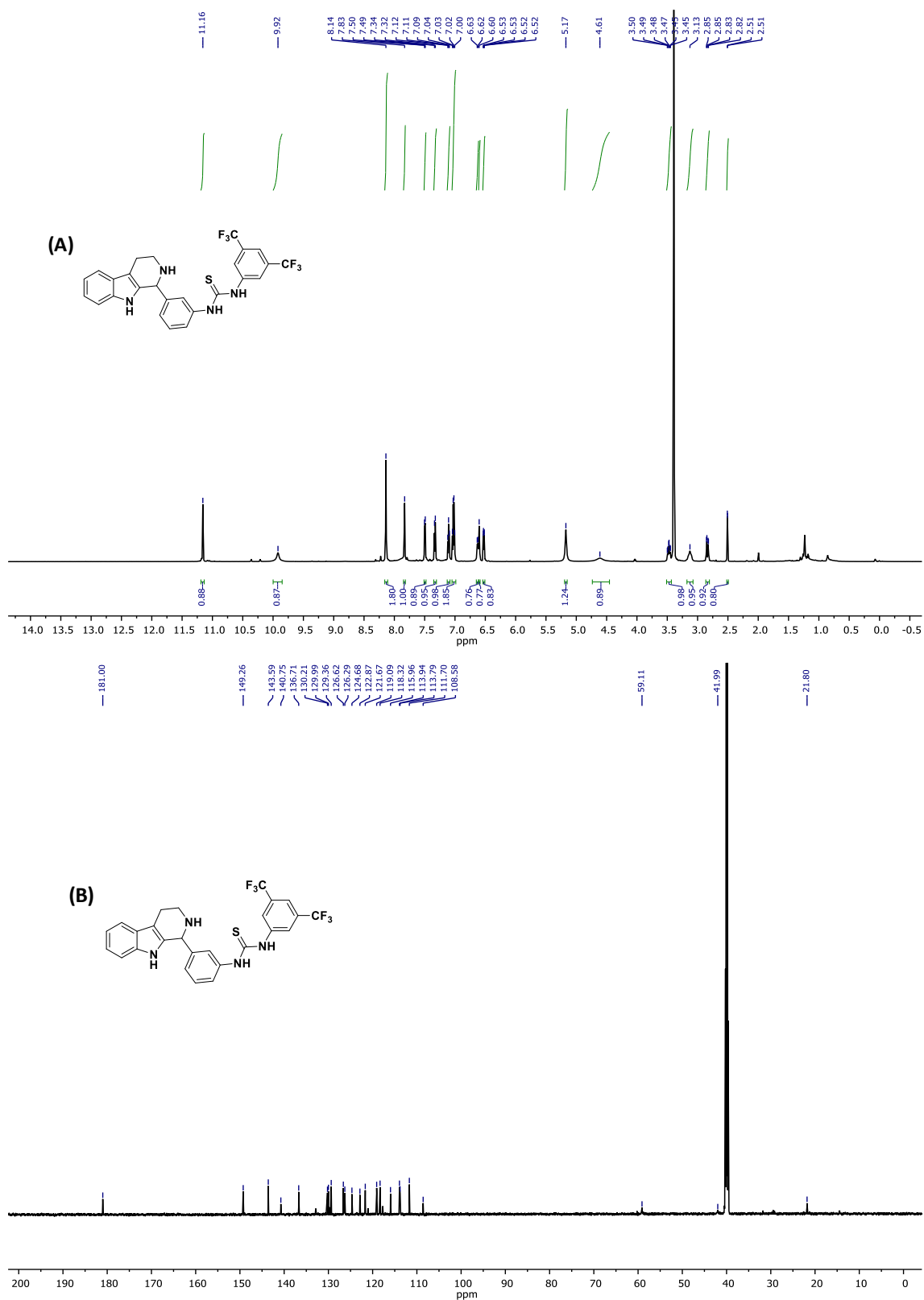


Fig. S29. ¹H NMR (A) and ¹³C NMR (B) spectra of 1-(3,5-bis(trifluoromethyl)phenyl)-3-(2,3,4,9-tetrahydro-1H-pyrido[3,4-b]indol-1-yl)phenylthiourea (**1b**) in the DMSO-*d*₆ solvent.

SUPPORTING INFORMATION

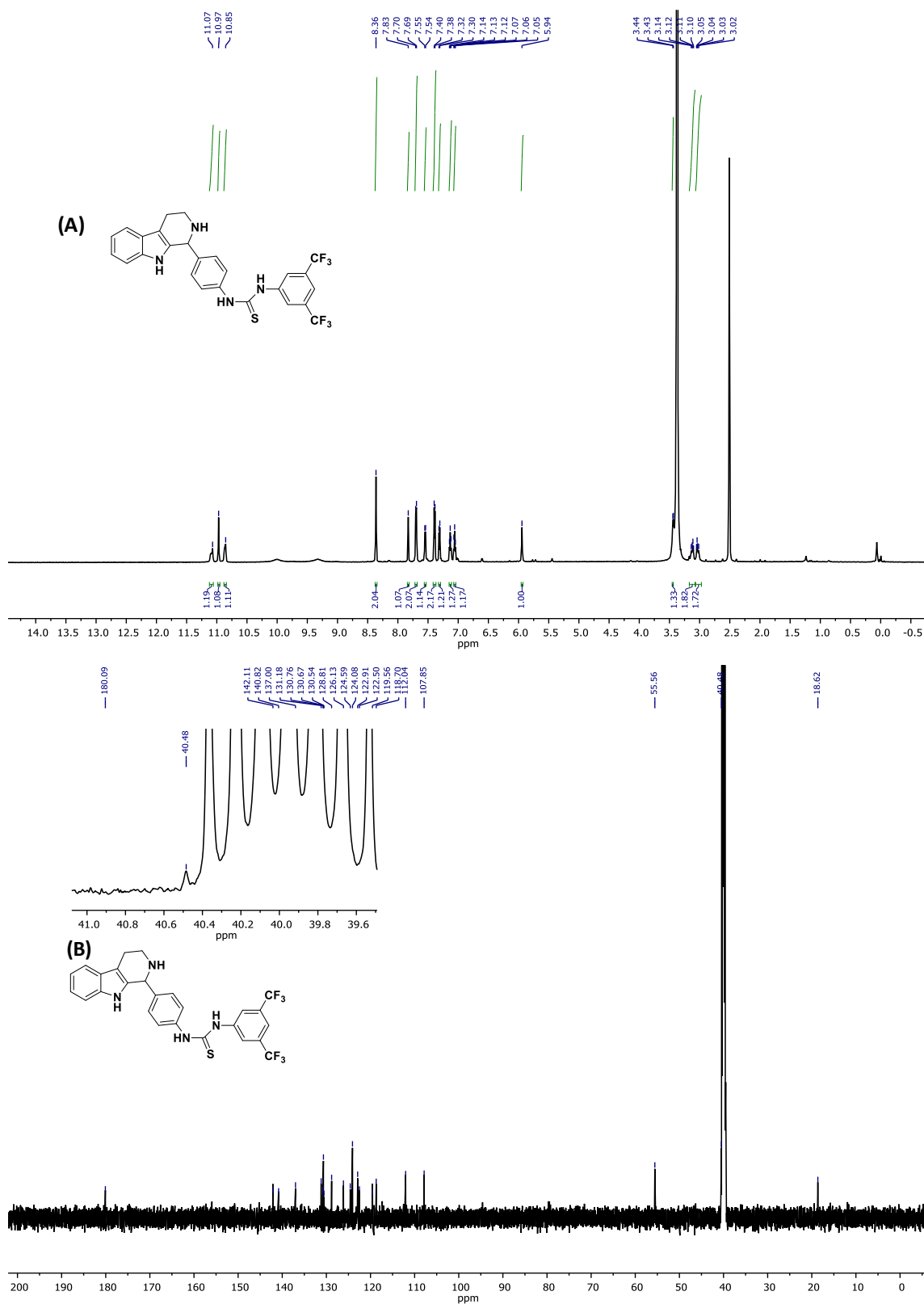


Fig. S30. ¹H NMR (A) and ¹³C NMR (B) spectra of 1-(3,5-bis(trifluoromethyl)phenyl)-3-(4-(2,3,4,9-tetrahydro-1H-pyrido[3,4-b]indol-1-yl)phenyl)thiourea (**1c**) in the DMSO-*d*₆ solvent.

SUPPORTING INFORMATION

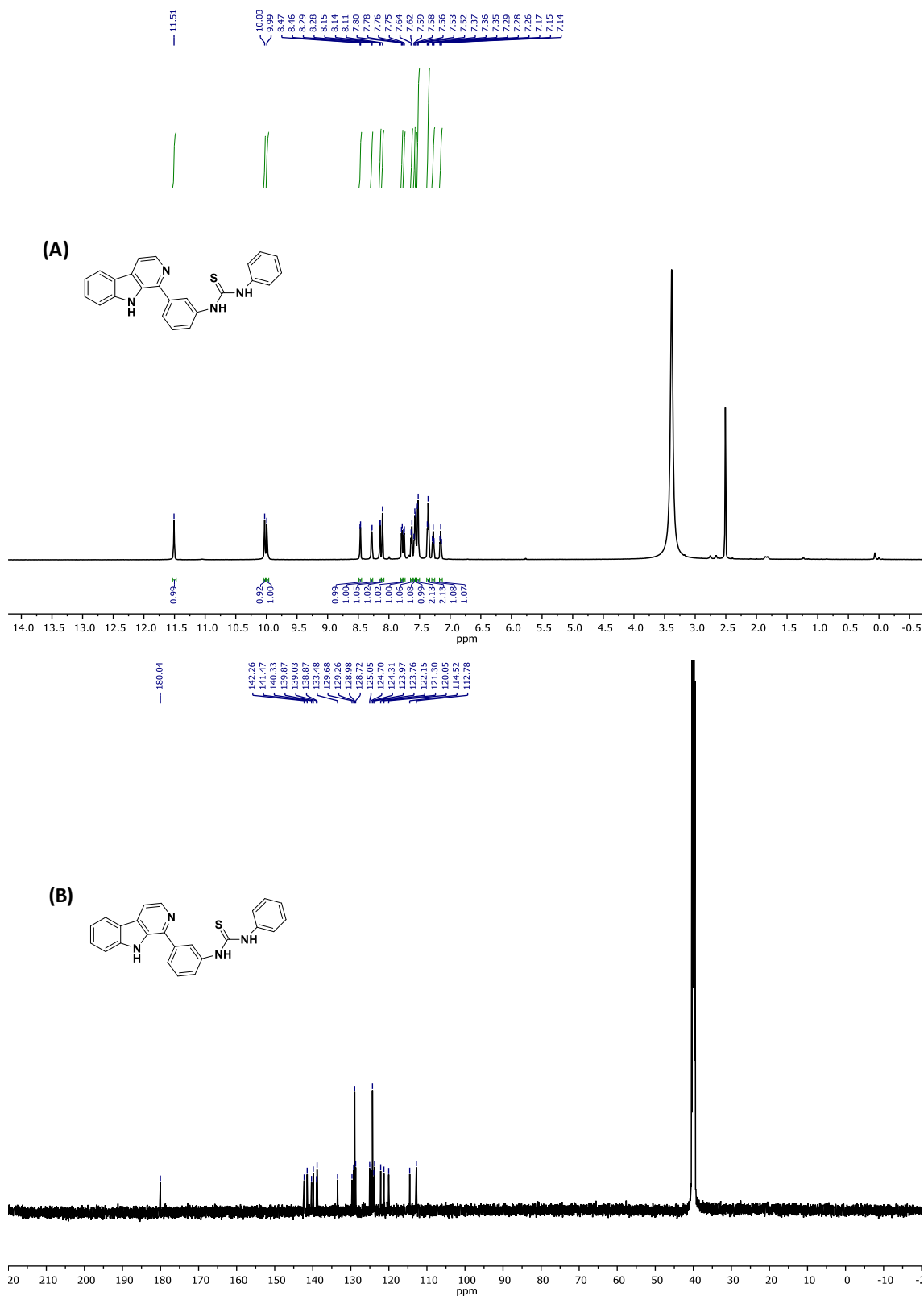


Fig. S31. ^1H NMR (A) and ^{13}C NMR (B) spectra of 1-(3-(9H-pyrido[3,4-b]indol-1-yl)phenyl)-3-phenylthiourea (**2**) in the $\text{DMSO-}d_6$ solvent.

SUPPORTING INFORMATION

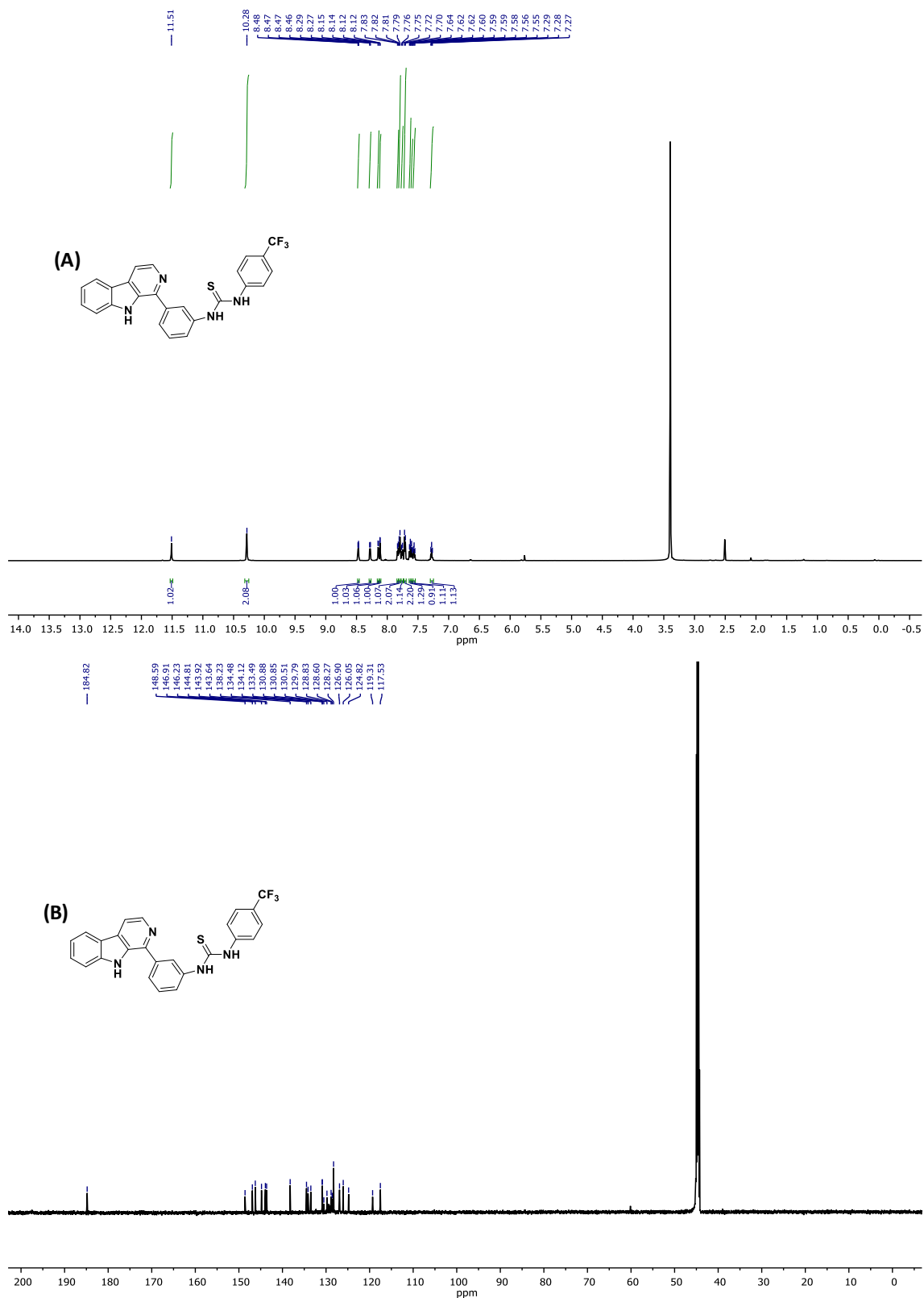


Fig. S32. ¹H NMR (A) and ¹³C NMR (B) spectra of 1-(3-(9H-pyrido[3,4-b]indol-1-yl)phenyl)-3-(4-(trifluoromethyl)phenyl)thiourea (3) in the DMSO-*d*₆ solvent.

SUPPORTING INFORMATION

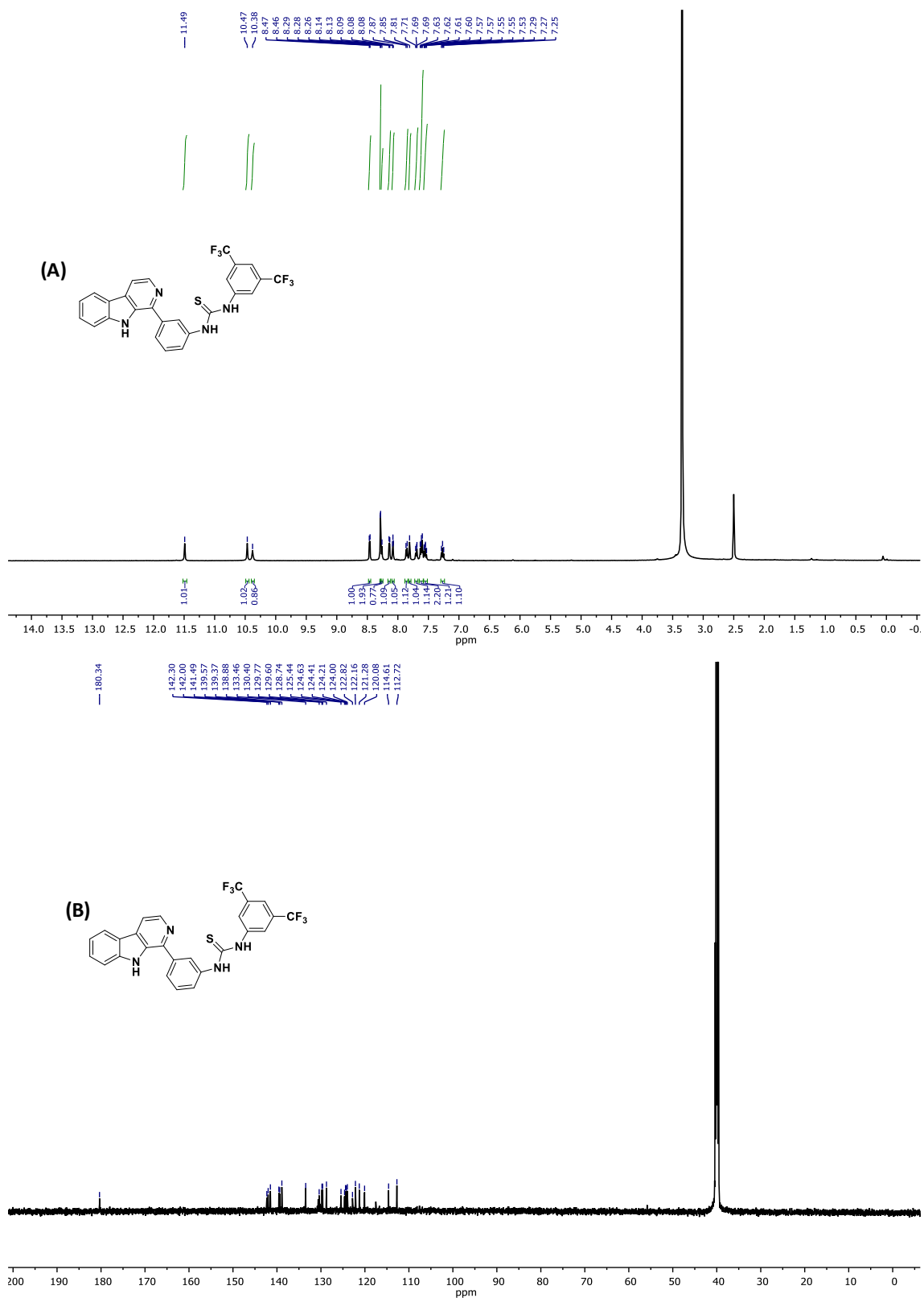


Fig. S33. ¹H NMR (A) and ¹³C NMR (B) spectra of 1-(3-(9H-pyrido[3,4-b]indol-1-yl)phenyl)-3-(3,5-bis(trifluoromethyl)phenyl)thiourea (**4a**) in the DMSO-*d*₆ solvent.

SUPPORTING INFORMATION

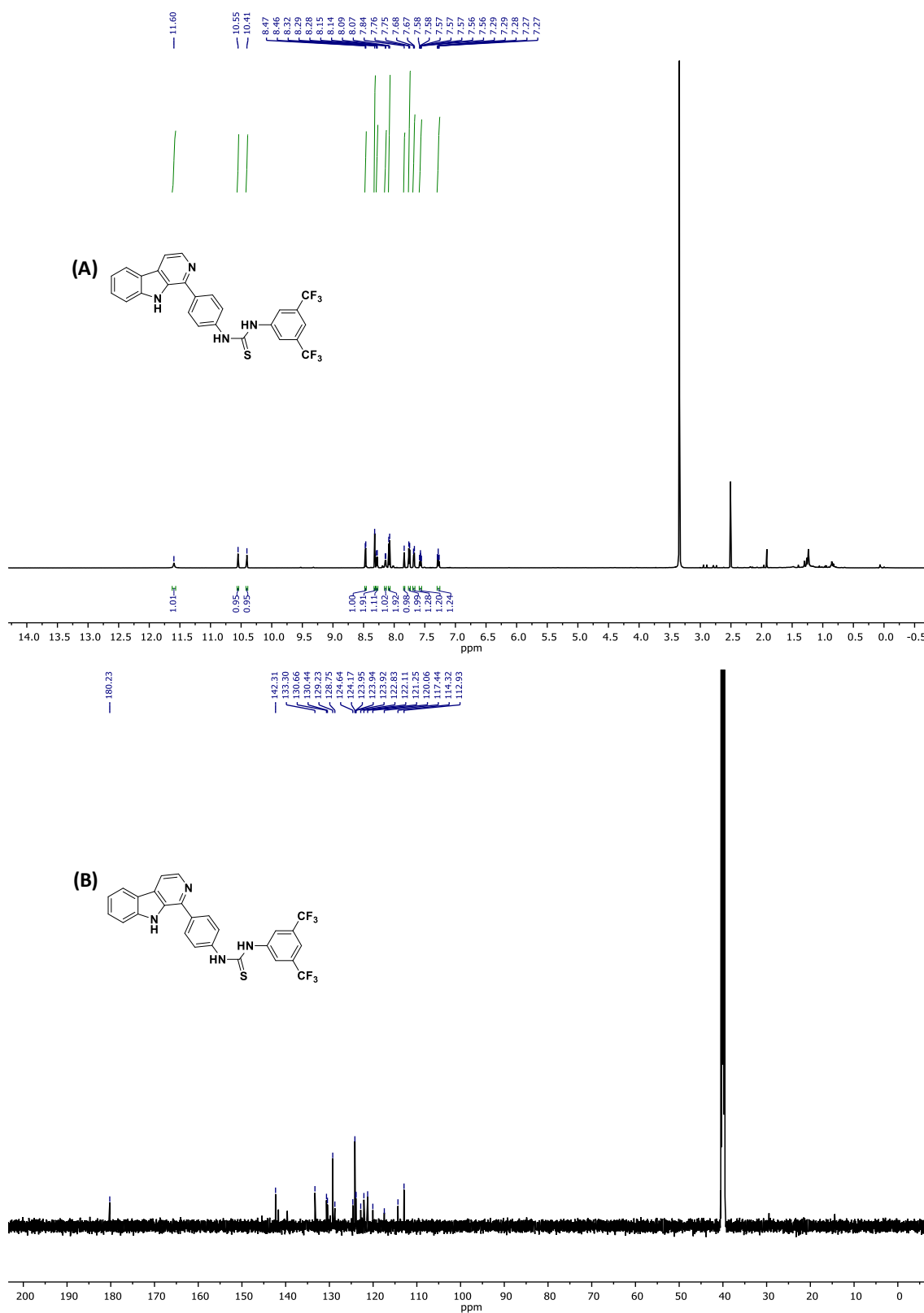


Fig. S34. ^1H NMR (A) and ^{13}C NMR (B) spectra of 1-(4-(9H-pyrido[3,4-b]indol-1-yl)phenyl)-3-(3,5-bis(trifluoromethyl)phenyl)thiourea (**4c**) in the DMSO- d_6 solvent.

SUPPORTING INFORMATION

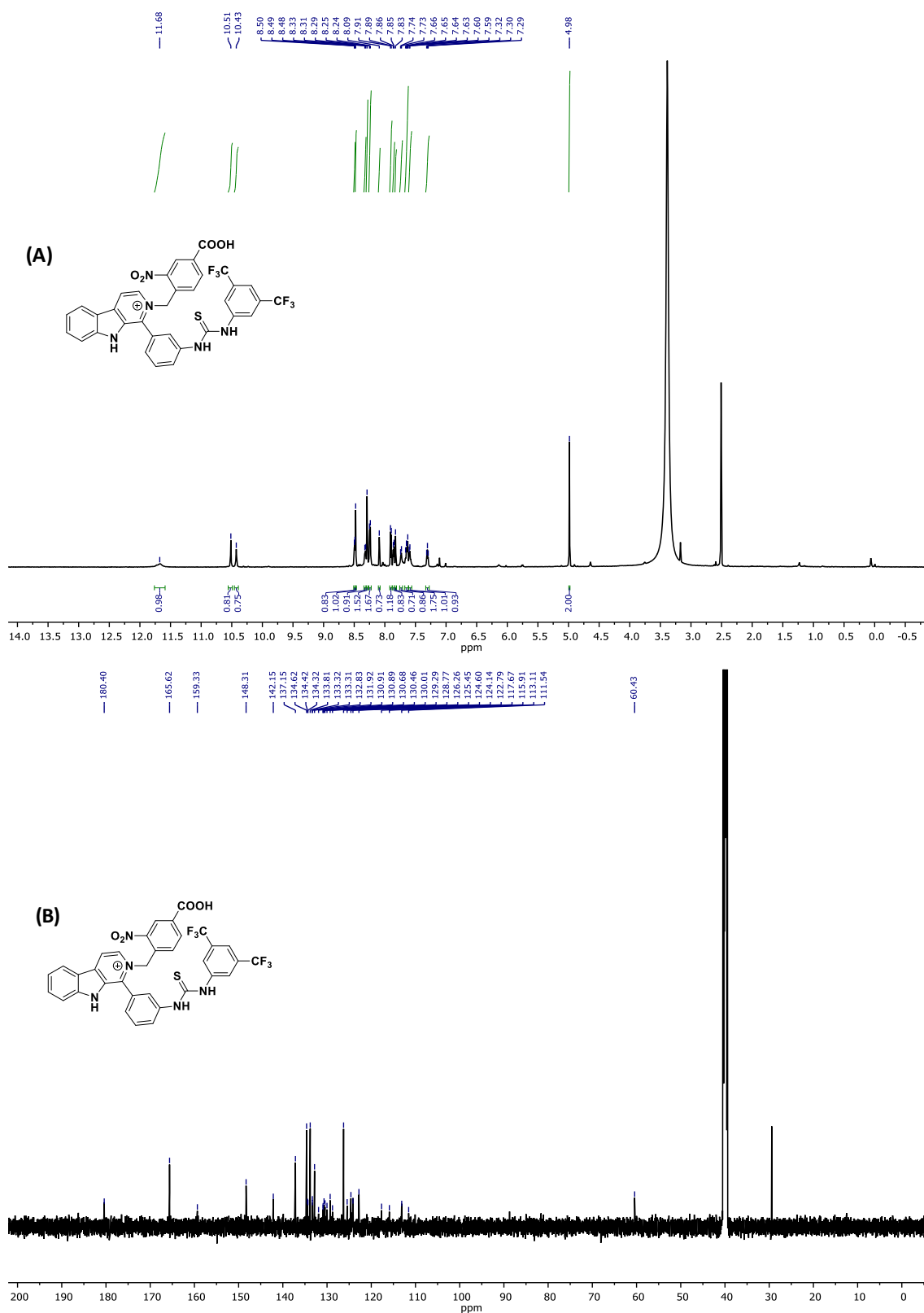


Fig. S35. ^1H NMR (A) and ^{13}C NMR (B) spectra of 1-(3-(3-(3,5-bis(trifluoromethyl)phenyl)thioureido)phenyl)-2-(4-carboxy-2-nitrobenzyl)-9H-pyrido[3,4-b]indol-2-ium (**5**) in the $\text{DMSO}-d_6$ solvent.

References.

1. Y. Zhang, Y. Li, X. Chen, X. Chen, C. Chen, L. Wang, X. Dong, G. Wang, R. Gu and F. Li, *J. Med. Chem.*, 2022, **65**, 11214-11228.
2. A. S. M. Arshad, R. Meesala, N. A. Hanapi and M. N. Mordi, *Tetrahedron*, 2021, **83**, 131960.
3. A. Saha, N. Akhtar, V. Kumar, S. Kumar, H. K. Srivastava, S. Kumar and D. Manna, *Org. Biomol. Chem.*, 2019, **17**, 5779-5788.
4. S. Srimayee, S. R. Badajena, N. Akhtar, M. K. Kar, S. Dey, P. Mohapatra and D. Manna, *ChemComm*, 2023, **59**, 12759-12762.
5. N. Akhtar, N. Pradhan, G. K. Barik, S. Chatterjee, S. Ghosh, A. Saha, P. Satpati, A. Bhattacharyya, M. K. Santra and D. Manna, *ACS Appl. Mater. Interfaces*, 2020, **12**, 25521-25533.
6. S. Das, R. Karn, M. Kumar, S. Srimayee and D. Manna, *Org. Biomol. Chem.*, 2024, **22**, 114-119.
7. H. Valkenier, L. W. Judd, H. Li, S. Hussain, D. N. Sheppard and A. P. Davis, *J. Am. Chem. Soc.*, 2014, **136**, 12507-12512.
8. D. Villaron, J. E. Bos, F. Kohl, S. Mommer, J. de Jong and S. J. Wezenberg, *J. Org. Chem.*, 2023, **88**, 11328-11334.
9. S. J. Wezenberg, L. J. Chen, J. E. Bos, B. L. Feringa, E. N. W. Howe, X. Wu, M. A. Siegler and P. A. Gale, *J. Am. Chem. Soc.*, 2022, **144**, 331-338.
10. N. Akhtar, N. Pradhan, A. Saha, V. Kumar, O. Biswas, S. Dey, M. Shah, S. Kumar and D. Manna, *Chem. Comm*, 2019, **55**, 8482-8485.
11. S. V. Shinde and P. Talukdar, *Chem. Comm*, 2018, **54**, 10351-10354.
12. O. Biswas, N. Akhtar, Y. Vashi, A. Saha, V. Kumar, S. Pal, S. Kumar and D. Manna, *ACS Appl. Bio Mater.*, 2020, **3**, 935-944.
13. J. A. Malla, A. Upadhyay, P. Ghosh, D. Mondal, A. Mondal, S. Sharma and P. Talukdar, *Org. Lett.*, 2022, **24**, 4124-4128.
14. A. D. Becke, *J. Chem. Phys.*, 1933, **98**, 5648-5652
15. K. Vanommeslaeghe, E. Hatcher, C. Acharya, S. Kundu, S. Zhong, J. Shim, E. Darian, O. Guvench, P. Lopes, I. Vorobyov and A. D. MacKerell, *J. Comput. Chem*, 2010, **31**, 671-690.
16. K. Vanommeslaeghe and A. D. MacKerell, *J. Chem. Inf. Model*, 2012, **52**, 3144-3154.

17. K. Vanommeslaeghe, E. P. Raman and A. D. MacKerell, *J. Chem. Inf. Model*, 2012, **52**, 3155-3168.
18. W. L. Jorgensen, J. Chandrasekhar, J. D. Madura, R. W. Impey and M. L. Klein, *J. Chem. Phys.*, 1983, **79**, 926-935.
19. S. Jo, T. Kim, V. G. Iyer and W. Im, *J. Comput. Chem.*, 2008, **29**, 1859-1865.
20. J. C. Phillips, R. Braun, W. Wang, J. Gumbart, E. Tajkhorshid, E. Villa, C. Chipot, R. D. Skeel, L. Kalé and K. Schulten, *J. Comput. Chem.*, 2005, **26**, 1781-1802.
21. J. C. Phillips, D. J. Hardy, J. D. C. Maia, J. E. Stone, J. V. Ribeiro, R. C. Bernardi, R. Buch, G. Fiorin, J. Hénin, W. Jiang, R. McGreevy, M. C. R. Melo, B. K. Radak, R. D. Skeel, A. Singharoy, Y. Wang, B. Roux, A. Aksimentiev, Z. Luthey-Schulten, L. V. Kale, K. Schulten, C. Chipot and E. Tajkhorshid, *J. Chem. Phys.*, 2020, **153**.
22. J. B. Klauda, R. M. Venable, J. A. Freites, J. W. O'Connor, D. J. Tobias, C. Mondragon-Ramirez, I. Vorobyov, A. D. MacKerell and R. W. Pastor, *J. Phys. Chem. B*, 2010, **114**, 7830-7843.
23. T. Darden, D. York and L. Pedersen, *J. Chem. Phys.*, 1993, **98**, 10089–10092.
24. G. J. Martyna, D. J. Tobias and M. L. Klein, *J. Chem. Phys.*, 1994, **101**, 4177-4189.
25. S. E. Feller, Y. H. Zhang, R. W. Pastor and B. R. Brooks, *J. Chem. Phys.*, 1995, **103**, 4613-4621.
26. M. Ahmad, N. J. Roy, A. Singh, D. Mondal, A. Mondal, T. Vijayakanth, M. Lahiri and P. Talukdar, *Chem. Sci*, 2023, **14**, 8897-8904.
27. S. Aaghaz, K. Sharma, R. Jain and A. Kamal, *Eur. J. Med. Chem.*, 2021, **216**, 113321.
28. N. Shankaraiah, S. Nekkanti, K. J. Chudasama, K. R. Senwar, P. Sharma, M. K. Jeengar, V. G. M. Naidu, V. Srinivasulu, G. Srinivasulu and A. Kamal, *Bioorg. Med. Chem. Lett.*, 2014, **24**, 5413-5417.